

SOURCES OF NON-EQUILIBRIUM IN PLASMA MATERIALS PROCESSING*

**Mark J. Kushner
University of Illinois
Dept. of Electrical and Computer Engineering
1406 W. Green St.
Urbana, IL 61801 USA
mjk@uiuc.edu <http://uigelz.ece.uiuc.edu>**

June 2003

*** Work supported by National Science Foundation, Semiconductor Research Corp., Electric Power Research Institute, Applied Materials.**

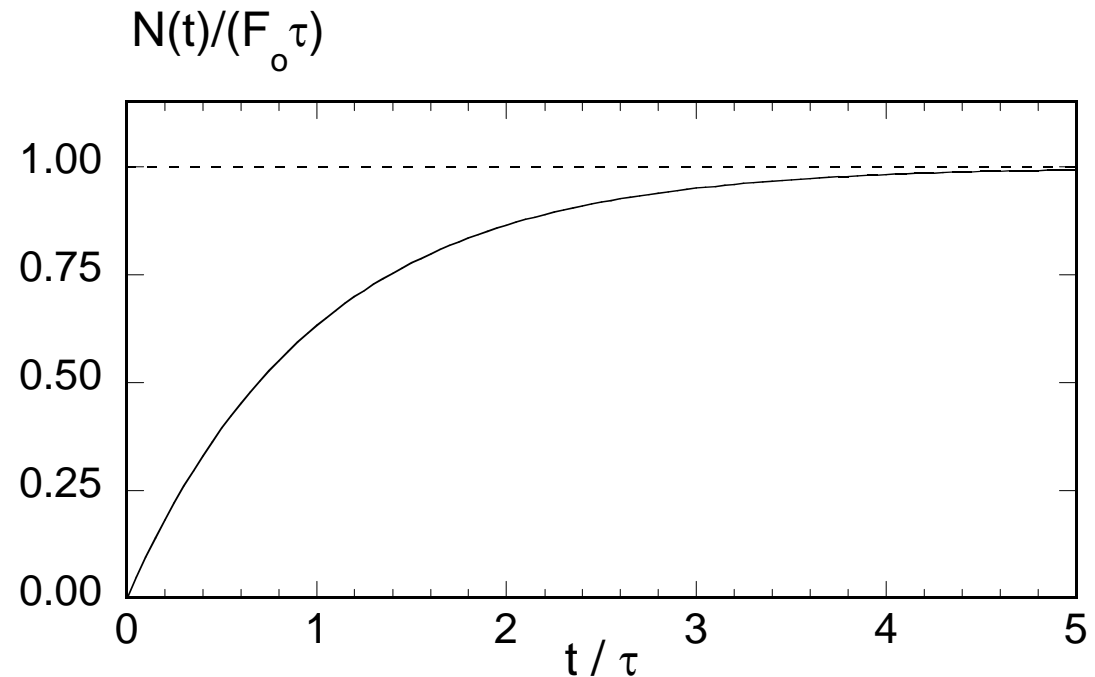
AGENDA

- **Sources of non-equilibrium in plasma processing**
- **Examples of non-equilibrium**
 - **Electron transport and electromagnetics**
 - **Wall chemistry and plasma kinetics**
 - **Electrostatics in microdischarges**
- **Concluding Remarks**

SO WHAT DO WE MEAN BY (NON-)EQUILIBRIUM?

- “Non-equilibrium” in plasma processing describes many phenomena, from electron transport to chemical kinetics.
- Mathematically.....If F is a source function for quantity $N(t)$ having damping constant τ , then...

$$\frac{dN(t)}{dt} = F_o - \frac{N(t)}{\tau}$$
$$N(t) = F_o \tau \left(1 - \exp\left(\frac{-t}{\tau}\right) \right)$$



NONEQUILIBRIUM IN ELECTRON TRANSPORT

- Electron transport is governed by Boltzmann's equation, which describes non-equilibrium evolution of EED in space and time.

$$\frac{df(\varepsilon, r, t)}{dt} = -\frac{q\vec{E}(r, t)}{m_e} \cdot \nabla_v f(\varepsilon, r, t) - \vec{v} \cdot \nabla f(\varepsilon, r, t) + \left(\frac{\partial f}{\partial t}\right)_c$$

- Should collisions and advection dominate, spatially dependent steady state time solutions are obtained.

$$\left|\left(\frac{\partial f}{\partial t}\right)_c\right| \approx \left|\frac{q\vec{E}}{m_e} \cdot \nabla_v f\right| \approx |\vec{v} \cdot \nabla f| \gg \left|\frac{df}{dt}\right|, \quad f = F(E(t), N(t))$$

- Solutions may be adiabatic to slow changes in electric field or densities of collision partners.

NONEQUILIBRIUM IN ELECTRON TRANSPORT

- When collisions dissipate energy (and momentum) in distances (or times) small compared to advection, the Local Field approximation is obtained.

$$\left| \left(\frac{\partial f}{\partial t} \right)_c \right| \approx \left| \frac{q\vec{E}}{m_e} \cdot \nabla_v f \right| \gg |\vec{v} \cdot \nabla f|, \quad f(\mathbf{r}) = F(E(\mathbf{r}), N(\mathbf{r}))$$

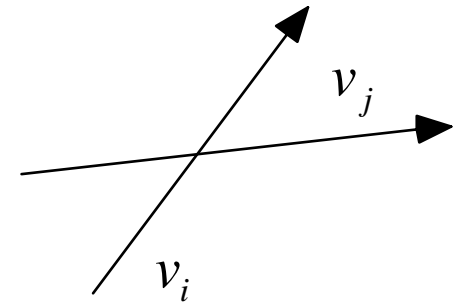
- Non-equilibrium is only manifested by changes in E and N.

NONEQUILIBRIUM IN NEUTRAL (ION) TRANSPORT

- Nonequilibrium in neutral flow often results from “slip” of directed momenta at low pressure .

$$\frac{\partial N_i}{\partial t} = -\nabla \cdot \phi_i + S_i, \quad \phi_i = \rho_i v_i / m_i$$

$$\frac{\partial(\rho_i v_i)}{\partial t} = -\nabla P_i - \nabla \cdot (\rho_i v_i v_i) - \nabla \cdot \tau - \sum_j f_{ij} \alpha_{ij} (v_i - v_j) + S_i$$



- If $\alpha_{ij} \gg |v/\Delta x|$, the velocities equilibrate and a single fluid results.

$$\frac{\partial N}{\partial t} = -\nabla \cdot \phi, \quad \phi = \rho v / m, \quad \rho = \sum_i \rho_i$$

$$\frac{\partial(\rho v)}{\partial t} = -\nabla P - \nabla \cdot (\rho v v) - \nabla \cdot \tau + S_i$$

$$\frac{\partial N_i}{\partial t} = -\nabla \cdot \phi_i, \quad \phi_i = N_i v - D_i N_o \nabla \left(\frac{N_i}{N_o} \right)$$

NONEQUILIBRIUM IN CHEMICAL KINETICS

- Nonequilibrium in chemical kinetics (i.e., the source function) results from reaction rates being slow compared to convection.

$$\frac{\partial N_i}{\partial t} = -\nabla \cdot \phi_i + S_i$$

$$S_i = -N_i \sum_j N_j k_{ij} + \sum_{j,l} N_j N_l k_{jl} + (\nabla \cdot \phi_i) \gamma_i - \sum_l (\nabla \cdot \phi_l) \beta_{il}$$

- If $S_i \gg N_i (v/\Delta x)$, densities become functions of only local thermodynamic parameters (EOS).

$$\frac{\partial N_o}{\partial t} = -\nabla \cdot N_o v, \quad N_i = f(N_o, T)$$

- Slowly varying boundary conditions such as wall passivation produce long term “nonequilibrium.”

NONEQUILIBRIUM IN ELECTROMAGNETICS

- Electromagnetics are governed by Maxwell's equations. In the frequency domain,

$$-\frac{1}{\mu} \left(\nabla (\nabla \cdot \bar{E}) + \nabla^2 \bar{E} \right) = \frac{\partial^2 (\epsilon \bar{E})}{\partial t^2} + \bar{J}_{plasma} + \bar{J}_{antenna}$$

- Although a quasi-steady harmonic state solution, non-equilibrium occurs through the consequences of E on plasma transport.

$$\begin{aligned} \nabla \cdot \bar{E} &= \rho / \epsilon_o = 0 && \text{"Equilibrium"} \\ &= \sum_i q_i \int (dN_i / dt) dt \neq 0 && \text{"Nonequilibrium"} \end{aligned}$$

- These terms most often produce electrostatic waves.

NONEQUILIBRIUM IN ELECTROMAGNETICS

- Nonequilibrium often occurs through the feedback between the E-fields, electron transport and plasma generated current.
- Currents which are linearly proportional to fields...equilibrium

$$\bar{J}_{plasma}(r,t) = \sigma(r,t)\bar{E}(r,t) = \sigma_o(r,t)\bar{E}(r) \exp(i\omega t + \phi(r))$$

- Currents which have complex relationships to electron (or ion transport) initiated at remote sites...nonequilibrium

$$\bar{J}_{plasma}(r,t) = \iint G(r,t,r',t')\sigma(r',t')\bar{E}(r',t')dr' dt' = \sum_i q_i(N_i v_i)$$

- In ICP systems, this results in non-monotonic decay of E-fields.

ELECTROSTATIC NONEQUILIBRIUM

- The self shielding of plasmas through the generation of self restoring electric fields provides “electrostatic” equilibrium.

$$\phi_i = -q_i \mu_i \nabla \Phi - D \nabla N_i \quad \leftrightarrow \quad -\nabla \cdot \epsilon \nabla \Phi = \sum_i q_i N_i$$

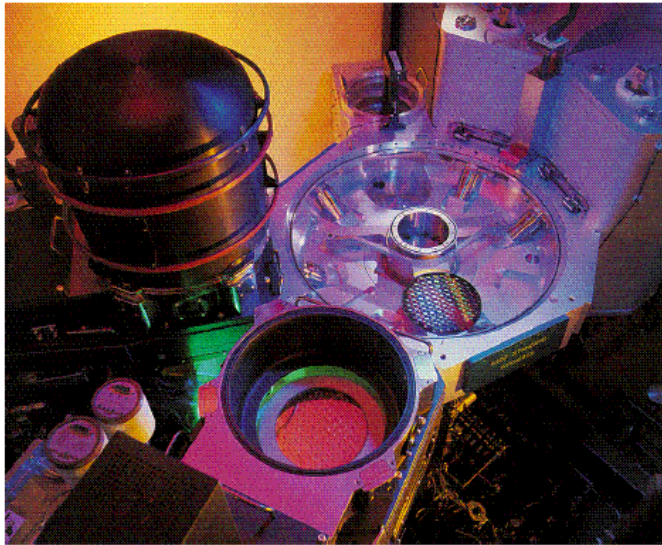
- Self restoring electric fields ultimately produce quasi-neutrality and ambipolar transport.

$$\sum_i q_i N_i \approx 0 \quad \rightarrow \quad \phi_i = D_{ambipolar} \nabla N_i$$

- In systems where dimensions are commensurate with Debye lengths and shielding is incomplete, electrostatic non-equilibrium occurs.

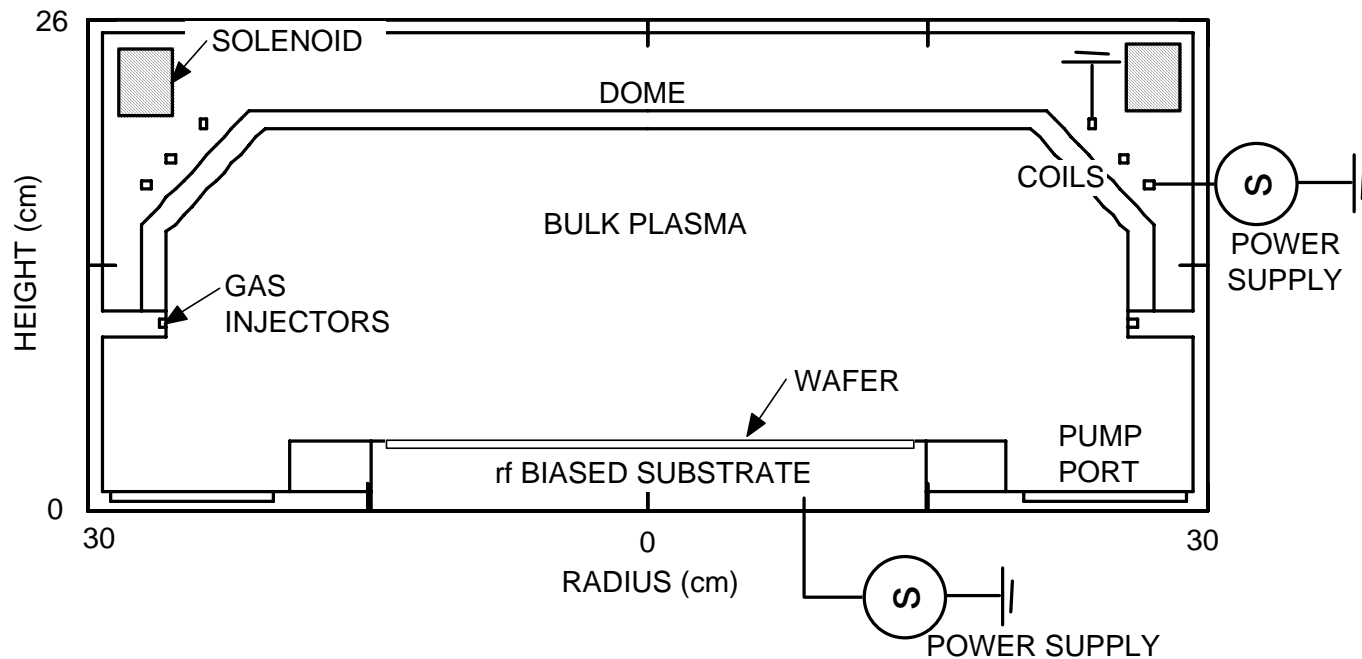
EXAMPLES OF NON-EQUILIBRIUM

- **Electromagnetic non-equilibrium: Anomalous skin depth**
- **Chemical non-equilibrium: Evolving wall passivation**
- **Electrostatic nonequilibrium: Microdischarges**



rf BIASED INDUCTIVELY COUPLED PLASMAS

- Inductively Coupled Plasmas (ICPs) with rf biasing are used here.
- $< 10\text{s mTorr}$, 10s MHz , $100\text{s W} - \text{kW}$, electron densities of $10^{11}\text{-}10^{12} \text{ cm}^{-3}$.



University of Illinois
Optical and Discharge Physics

ELECTROMAGNETICS MODEL

- The wave equation is solved in the frequency domain with tensor conductivities.

$$-\nabla \cdot \left(\frac{1}{\mu} \nabla \cdot \bar{E} \right) + \nabla \cdot \left(\frac{1}{\mu} \nabla \bar{E} \right) = \frac{\partial^2 (\epsilon \bar{E})}{\partial t^2} + \frac{\partial (\bar{\sigma} \cdot \bar{E} + \bar{J})}{\partial t}$$

- The electrostatic term is addressed using a perturbation to the electron density.

$$\nabla \cdot \bar{E} = \frac{\rho}{\epsilon} = \frac{q \Delta n_e}{\epsilon}, \quad \Delta n_e = -\nabla \cdot \left(\frac{\bar{\sigma} \cdot \bar{E}}{q} \right) / \left(\frac{1}{\tau} + i\omega \right)$$

- Conduction currents are kinetically derived to account for non-collisional effects.

$$J_e(\vec{r}, t) = J_o(\vec{r}) \exp(i(\omega t + \phi_v(\vec{r}))) = -q n_e(\vec{r}) \vec{v}_e(\vec{r}) \exp(i(\omega t + \phi_v(\vec{r})))$$

ELECTRON ENERGY TRANSPORT

- **Continuum:**

$$\partial \left(\frac{3}{2} n_e k T_e \right) / \partial t = S(T_e) - L(T_e) - \nabla \cdot \left(\frac{5}{2} \Phi k T_e - \bar{\kappa}(T_e) \cdot \nabla T_e \right) + S_{EB}$$

where $S(T_e)$	=	Power deposition from electric fields
$L(T_e)$	=	Electron power loss due to collisions
Φ	=	Electron flux
$\kappa(T_e)$	=	Electron thermal conductivity tensor
S_{EB}	=	Power source source from beam electrons

- **Kinetic:** A Monte Carlo Simulation is used to derive $f(\varepsilon, \vec{r}, t)$ including electron-electron collisions using electromagnetic and electrostatic fields.

PLASMA CHEMISTRY, TRANSPORT AND ELECTROSTATICS

- Continuity, momentum and energy equations for each species, and site balance models for surface chemistry.

$$\frac{\partial N_i}{\partial t} = -\nabla \cdot (N_i \vec{v}_i) + S_i$$

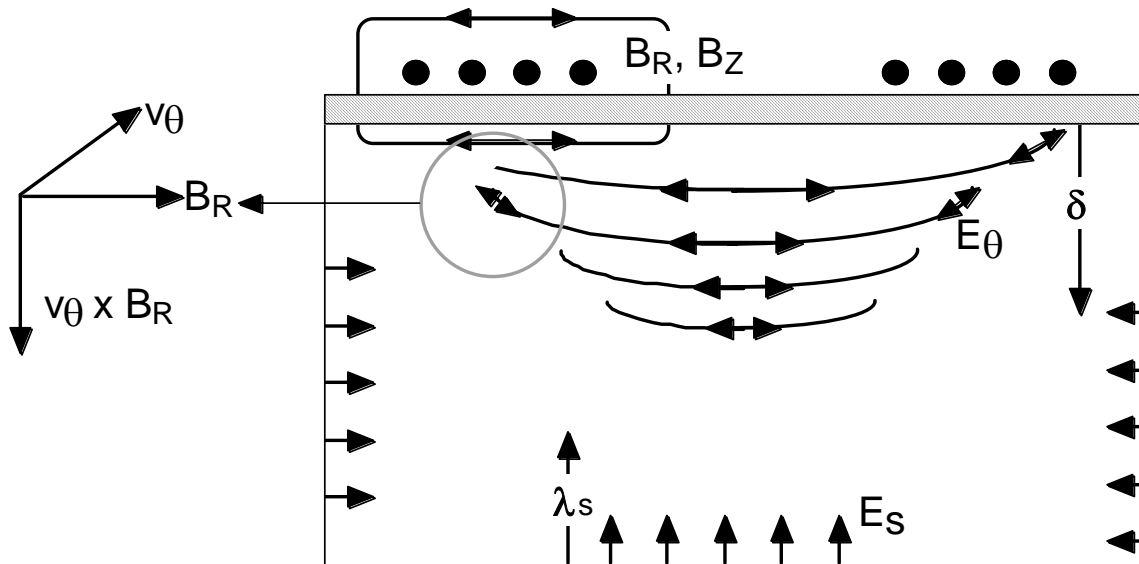
$$\frac{\partial (N_i \vec{v}_i)}{\partial t} = \frac{1}{m_i} \nabla (k N_i T_i) - \nabla \cdot (N_i \vec{v}_i \vec{v}_i) + \frac{q_i N_i}{m_i} (\vec{E} + \vec{v}_i \times \vec{B}) - \nabla \cdot \bar{\mu}_i - \sum_j \frac{m_j}{m_i + m_j} N_i N_j (\vec{v}_i - \vec{v}_j) \nu_{ij}$$

$$\begin{aligned} \frac{\partial (N_i \varepsilon_i)}{\partial t} + \nabla \cdot \mathbf{Q}_i + P_i \nabla \cdot \mathbf{U}_i + \nabla \cdot (N_i \mathbf{U}_i \varepsilon_i) &= \frac{N_i q_i^2 \nu_i}{m_i (\nu_i^2 + \omega^2)} E^2 \\ &+ \frac{N_i q_i^2}{m_i \nu_i} E_s^2 + \sum_j 3 \frac{m_{ij}}{m_i + m_j} N_i N_j R_{ij} k_B (T_j - T_i) \pm \sum_j 3 N_i N_j R_{ij} k_B T_j \end{aligned}$$

- Implicit solution of Poisson's equation.

$$\nabla \cdot \varepsilon \nabla \Phi(t + \Delta t) = - \left(\rho_s + \sum_i q_i N_i - \Delta t \cdot \sum_i \left(q_i \nabla \cdot \vec{\phi}_i \right) \right)$$

FORCES ON ELECTRONS IN ICPs



- Inductive E-field provides azimuthal acceleration; depth 1-3 cm.

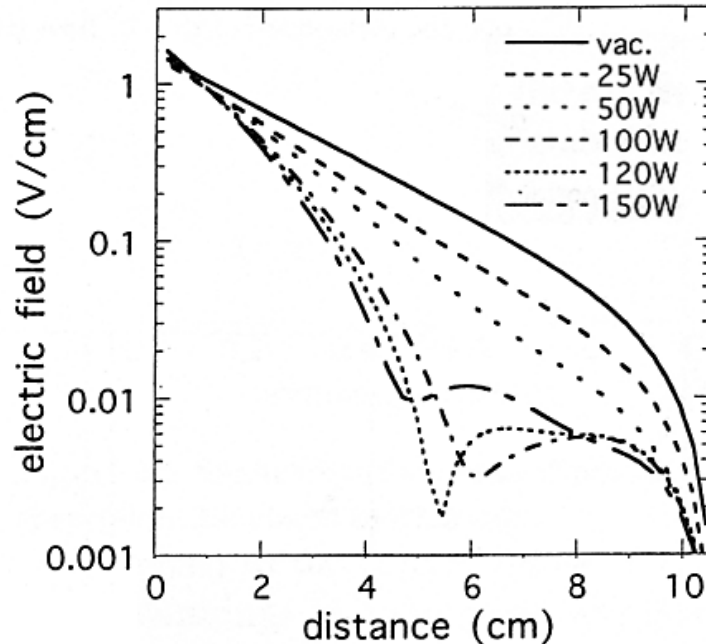
$$\delta = \left(m_e / (e^2 \mu_o n_e) \right)^{1/2}$$

- Electrostatic (capacitive) penetrates (100s μm to mm)

$$\lambda_s \approx 10 \lambda_D, \lambda_D = \left(kT_e / (8\pi n_e e^2) \right)^{1/2}$$

- Non-linear Lorentz Force $\vec{F} = v_\theta \times \vec{B}_{rf}$

ANAMOLOUS SKIN EFFECT AND POWER DEPOSITION



- Collisional heating:

$$\lambda_{mfp} < \delta_{skin}, \quad \vec{J}_e(\vec{r}, t) = \sigma(\vec{r}, t) \vec{E}(\vec{r}, t)$$

- Anomalous skin effect:

$$\lambda_{mfp} > \delta_{skin}$$

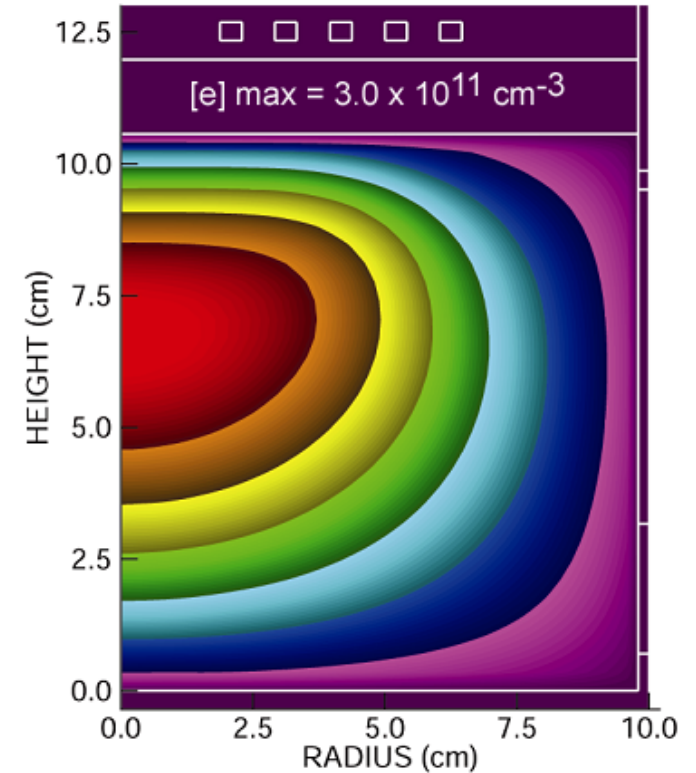
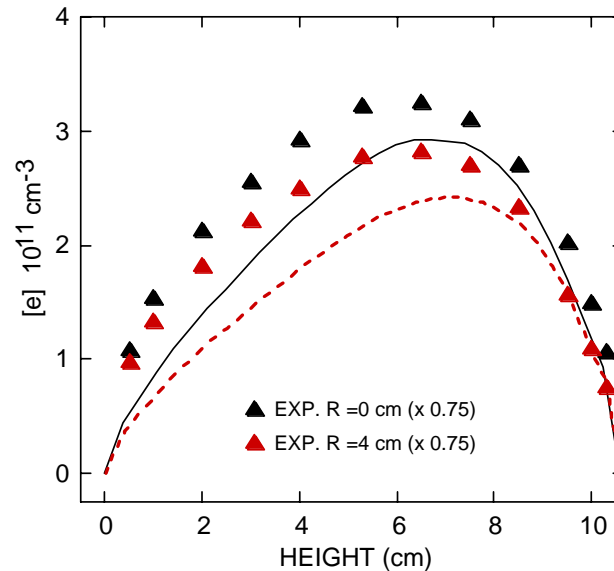
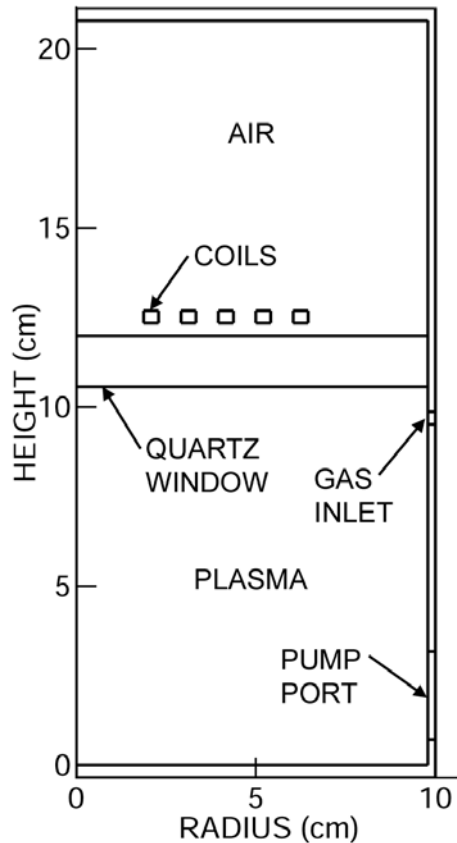
$$\vec{J}_e(\vec{r}, t) = \iint \sigma(\vec{r}, \vec{r}', t, t') \vec{E}(\vec{r}', t') d\vec{r}' dt'$$

$$\vec{F} = \vec{v} \times \vec{B}$$

- Ref: V. Godyak, “Electron Kinetics of Glow Discharges”

- Electrons receive (positive) and deliver (negative) power from/to the E-field.
- E-field is non-monotonic.

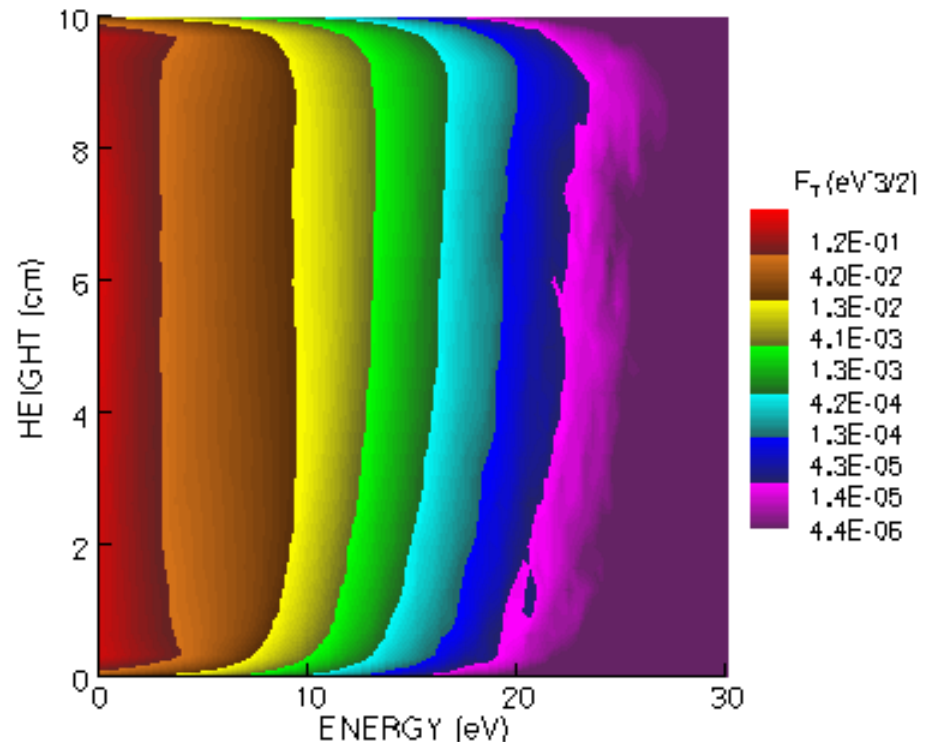
ELECTRON DENSITY: Ar, 10 mTorr, 200 W, 7 MHz



- **Model is about 20% below experiments. This likely has to do with details of the sheath model.**
- **V. Godyak et al, J. Appl. Phys. 85, 703 (1999); private communication**

TIME DEPENDENCE OF THE EED

- Time variation of the EED is mostly at higher energies where electrons are more collisional.
- Dynamics are dominantly in the electromagnetic skin depth where both collisional and non-linear Lorentz Forces) peak.
- The second harmonic dominates these dynamics.



- Ar, 10 mTorr, 100 W, 7 MHz, $r = 4$ cm

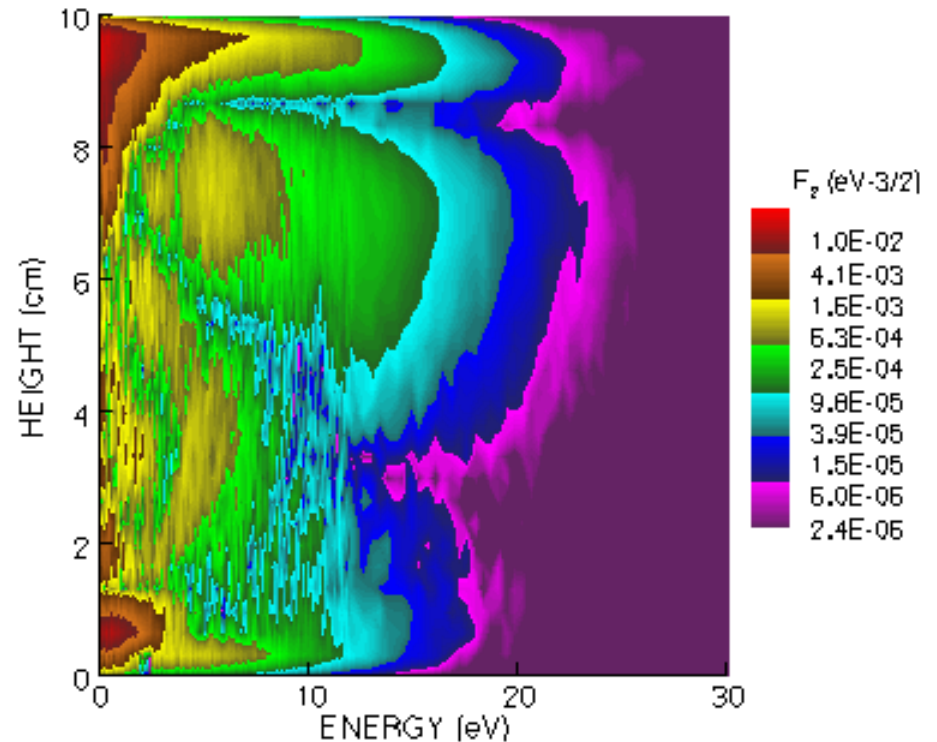
ANIMATION SLIDE

University of Illinois
Optical and Discharge Physics

TIME DEPENDENCE OF THE EED: 2nd HARMONIC

- Electrons in skin depth quickly increase in energy and are “launched” into the bulk plasma.
- Undergoing collisions while traversing the reactor, they degrade in energy.
- Those surviving “climb” the opposite sheath, exchanging kinetic for potential energy.
- Several “pulses” are in transit simultaneously.
- **Electron transport nonequilibrium!**

- Ar, 10 mTorr, 100 W, 7 MHz, $r = 4$ cm



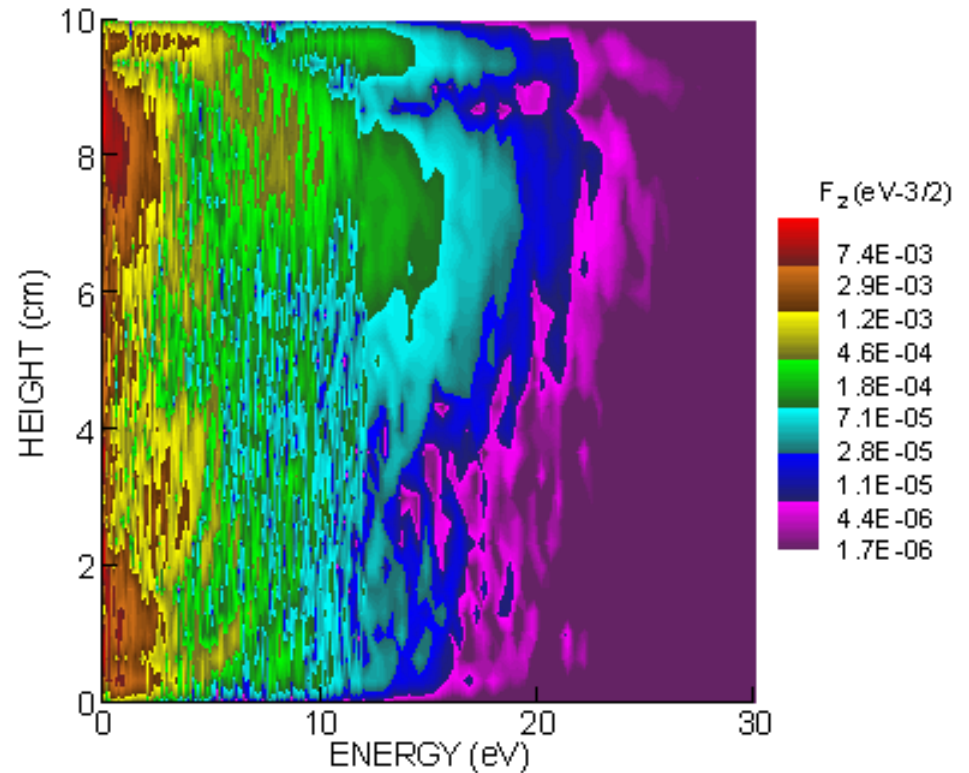
- Amplitude of 2nd Harmonic

ANIMATION SLIDE

University of Illinois
Optical and Discharge Physics

2nd HARMONIC OF EED WITHOUT LORENTZ FORCE

- Excluding $v \times B$ terms, the non-linear Lorentz Force is removed.
- Electrons are alternately heated and cooled in the skin depth, out of phase with E_{θ} , with some collisional heating.
- High energy electrons do not propagate (other than by diffusion) outside the skin layer.



- Amplitude of 2nd Harmonic

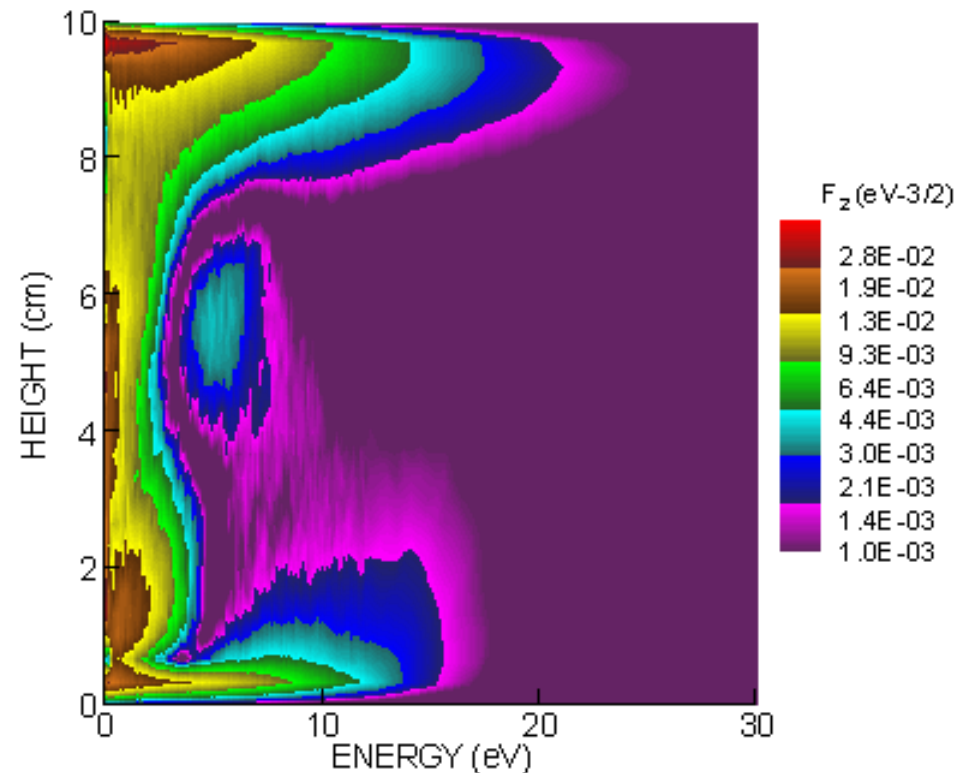
- Ar, 10 mTorr, 100 W, 7 MHz, $r = 4$ cm

ANIMATION SLIDE

University of Illinois
Optical and Discharge Physics

2nd HARMONIC OF EED: 1 mTorr, 3 MHz

- By decreasing frequency, B_{rf} increases, the skin depth lengthens and NLF increases.
- Lower pressure extends the electron mean free path.
- Significant modulation extends to lower energies.



- Amplitude of 2nd Harmonic

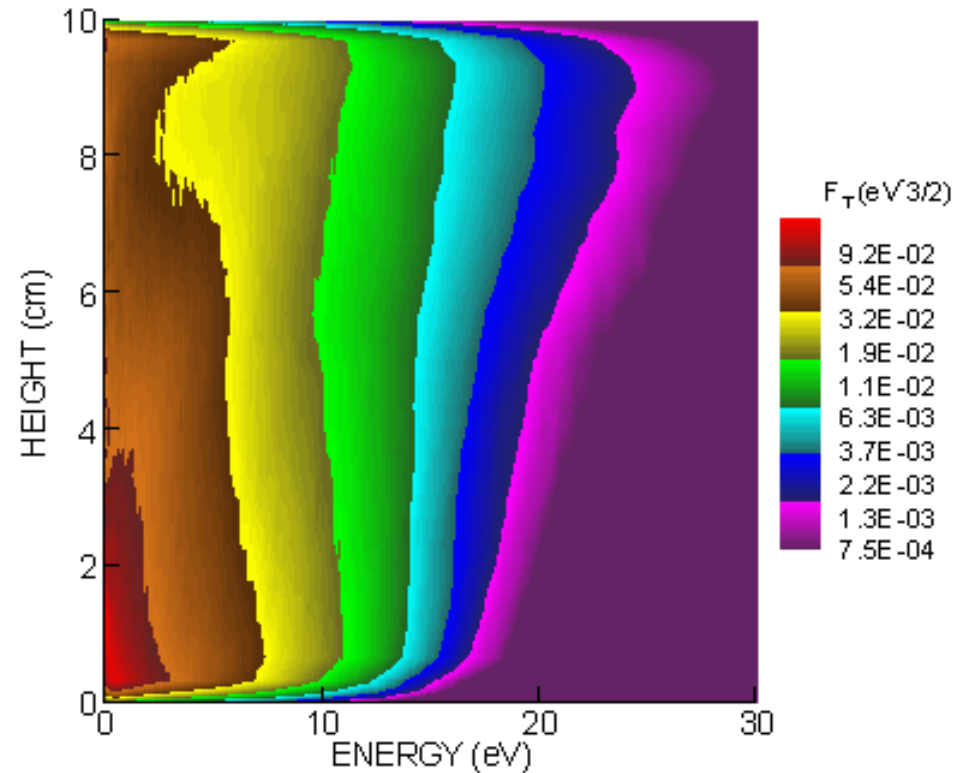
ANIMATION SLIDE

- Ar, 1 mTorr, 100 W, 3 MHz, $r = 4$ cm

University of Illinois
Optical and Discharge Physics

TIME DEPENDENCE OF EED: 1 mTorr, 3 MHz

- At reduced pressure and frequency, the conditions for the nonlinear skin effect are fulfilled.
- The EED is essentially depleted of low energy electrons in the skin layer.



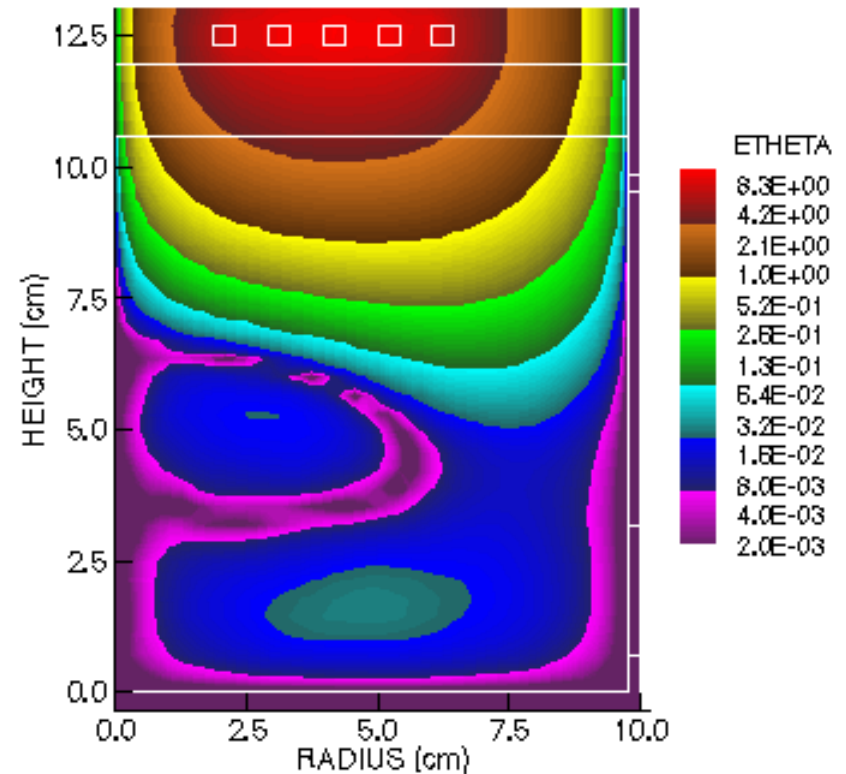
ANIMATION SLIDE

- Ar, 1 mTorr, 100 W, 3 MHz, $r = 4$ cm

University of Illinois
Optical and Discharge Physics

COLLISIONLESS TRANSPORT ELECTRIC FIELDS

- E_θ exhibits extrema and nodes resulting from this non-collisional transport.
- “Sheets” of electrons with different phases provide current sources interfering or reinforcing the electric field for the next sheet.
- Axial transport results from $\vec{v} \times \vec{B}_{rf}$ forces.
- **Electromagnetic nonequilibrium!**



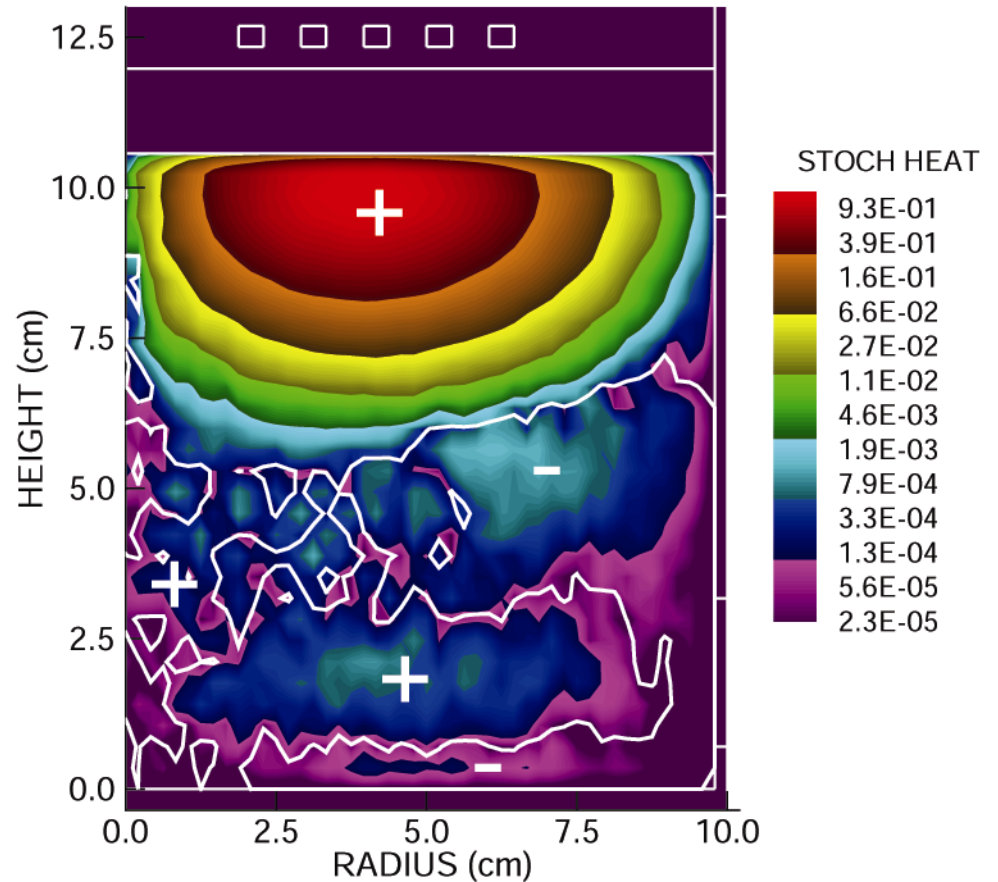
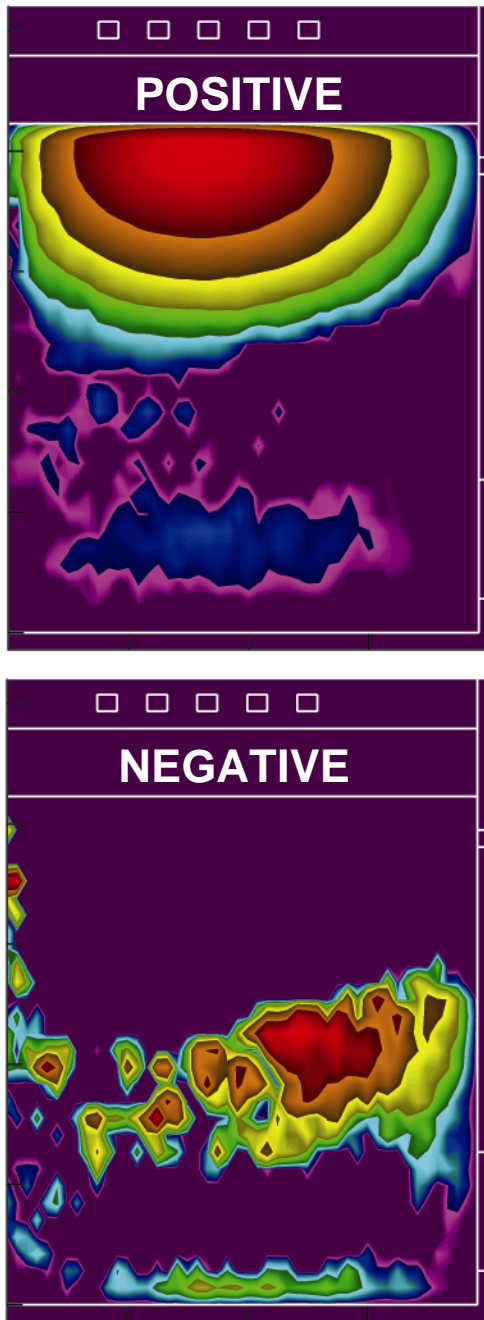
ANIMATION SLIDE

- Ar, 10 mTorr, 7 MHz, 100 W

University of Illinois
Optical and Discharge Physics

POWER DEPOSITION: POSITIVE AND NEGATIVE

- The end result is regions of positive and negative power deposition.

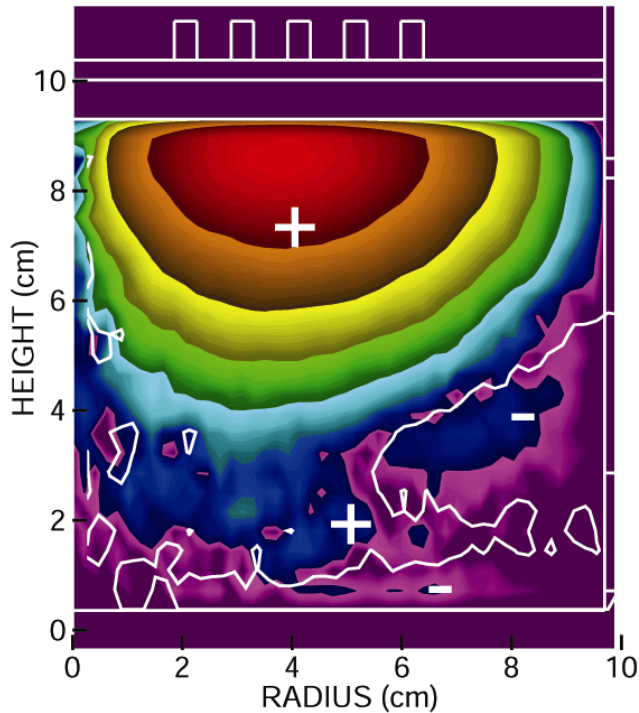


- Ar, 10 mTorr,
7 MHz, 100 W

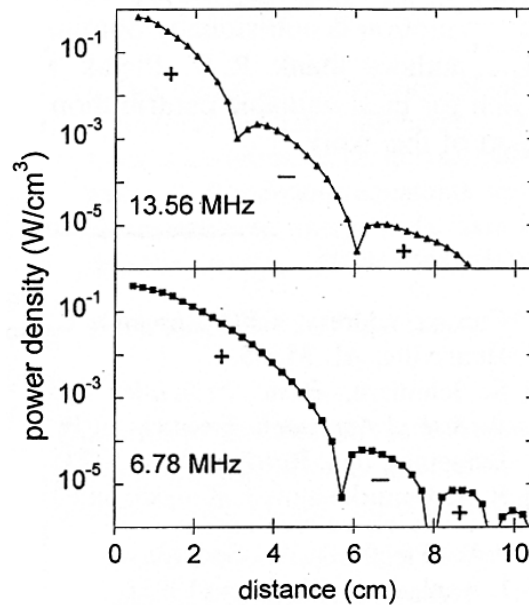
University of Illinois
Optical and Discharge Physics

POWER DEPOSITION vs FREQUENCY

- The shorter skin depth at high frequency produces more layers of negative power deposition of larger magnitude.

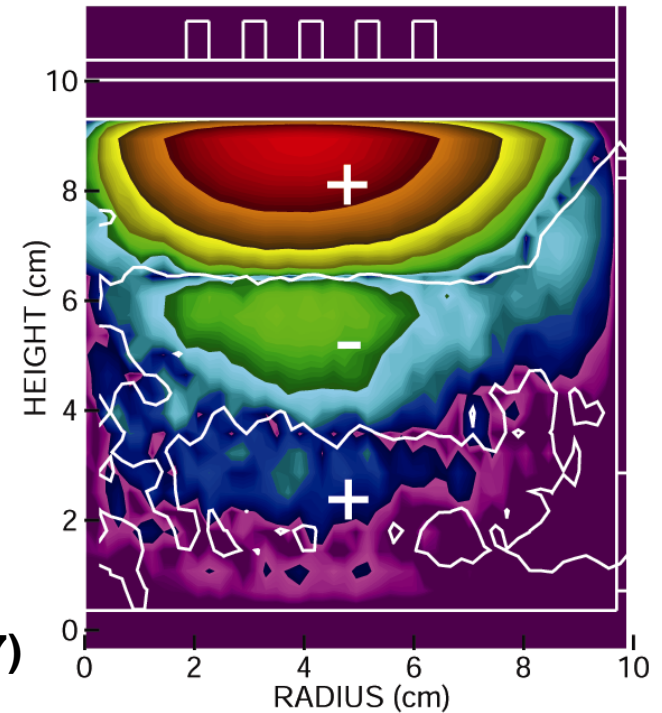


• **6.7 MHz**
 ($5 \times 10^{-5} - 1.4 \text{ W/cm}^3$)



• Ref: Godyak, PRL (1997)

• Ar, 10 mTorr, 200 W

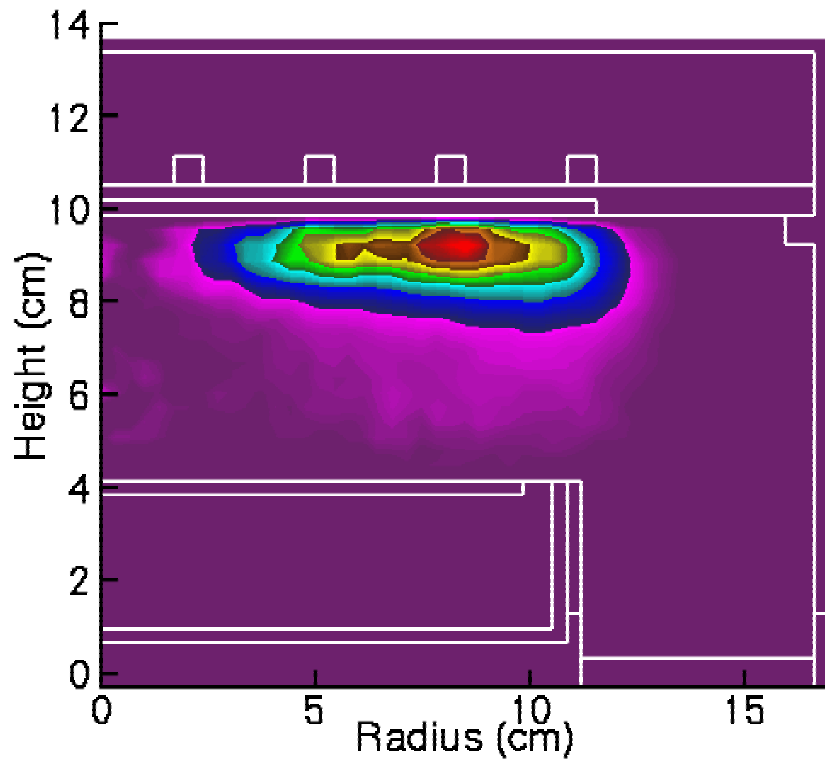


• **13.4 MHz**
 ($8 \times 10^{-5} - 2.2 \text{ W/cm}^3$)



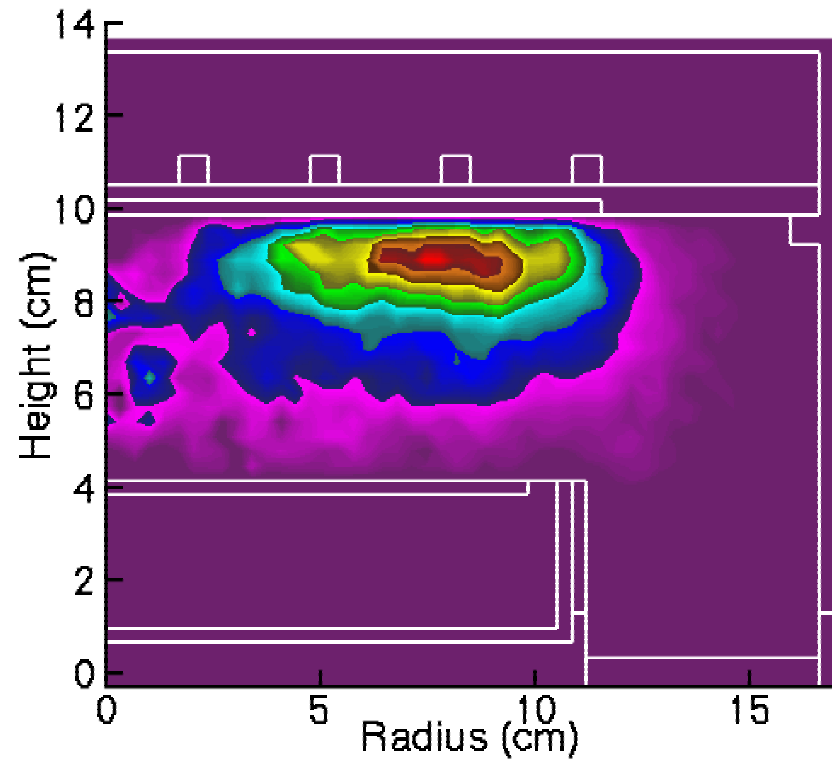
TIME DEPENDENCE OF Ar IONIZATION: PRESSURE

- Although B_{rf} may be nearly the same, at large P , v_0 and mean-free-paths are smaller, leading to lower harmonic amplitudes.



• 5 mTorr

$6 \times 10^{14} - 3 \times 10^{16} \text{ cm}^{-3}\text{s}^{-1}$



• 20 mTorr

$1.5 \times 10^{14} - 1.7 \times 10^{16} \text{ cm}^{-3}\text{s}^{-1}$

• Ar/N₂=60/40, 10 MHz

ANIMATION SLIDE

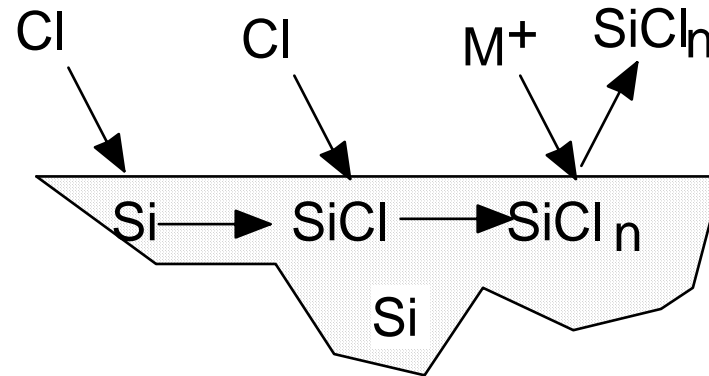
MIN  MAX

EXAMPLES OF NON-EQUILIBRIUM

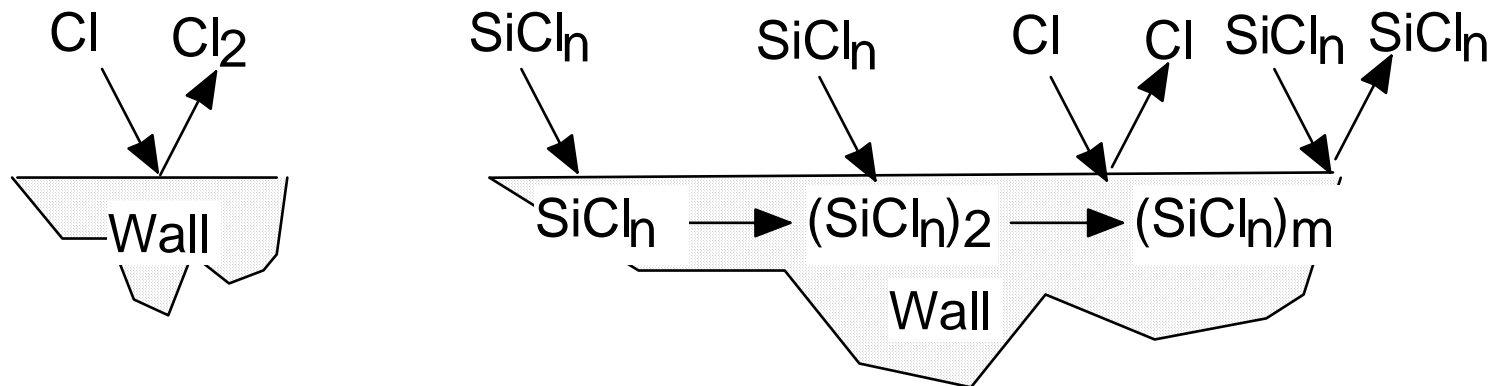
- **Electromagnetic non-equilibrium: Anomalous skin depth**
- **Chemical non-equilibrium: Evolving wall passivation**
- **Electrostatic nonequilibrium: Microdischarges**

SURFACE CHEMISTRY OF Si ETCHING IN Cl₂ PLASMAS

- Etching of Si in Cl₂ plasmas proceeds by passivation of Si sites, followed by ion activated removal of SiCl_n etch product.

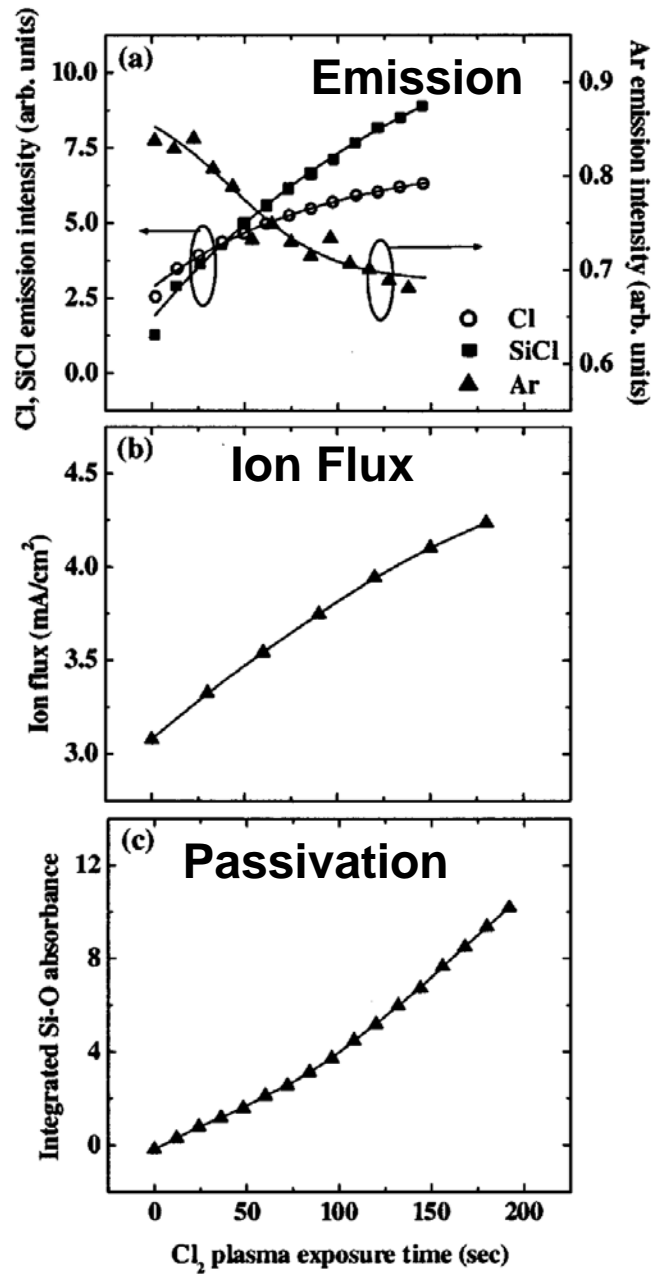


- Etch products deposit on reactor walls. Cl atom recombination and SiCl_n sticking slows on the passivated surfaces.



University of Illinois
Optical and Discharge Physics

LONG TERM PASSIVATION OF WALLS



- Experimental measurements of optical emission, ion flux and etch rates during Cl etching of Si have long term behavior.
- Transients are correlated with increasing film thickness on walls, reducing sticking coefficients for Cl and SiCl.
- ICP, Cl₂, 10 mTorr, 800 W.
- **Plasma-surface chemical nonequilibrium!**
- S. J. Ullal, T. W. Kim, V. Vahedi and E. S. Aydil, JVSTA 21, 589 (2003)

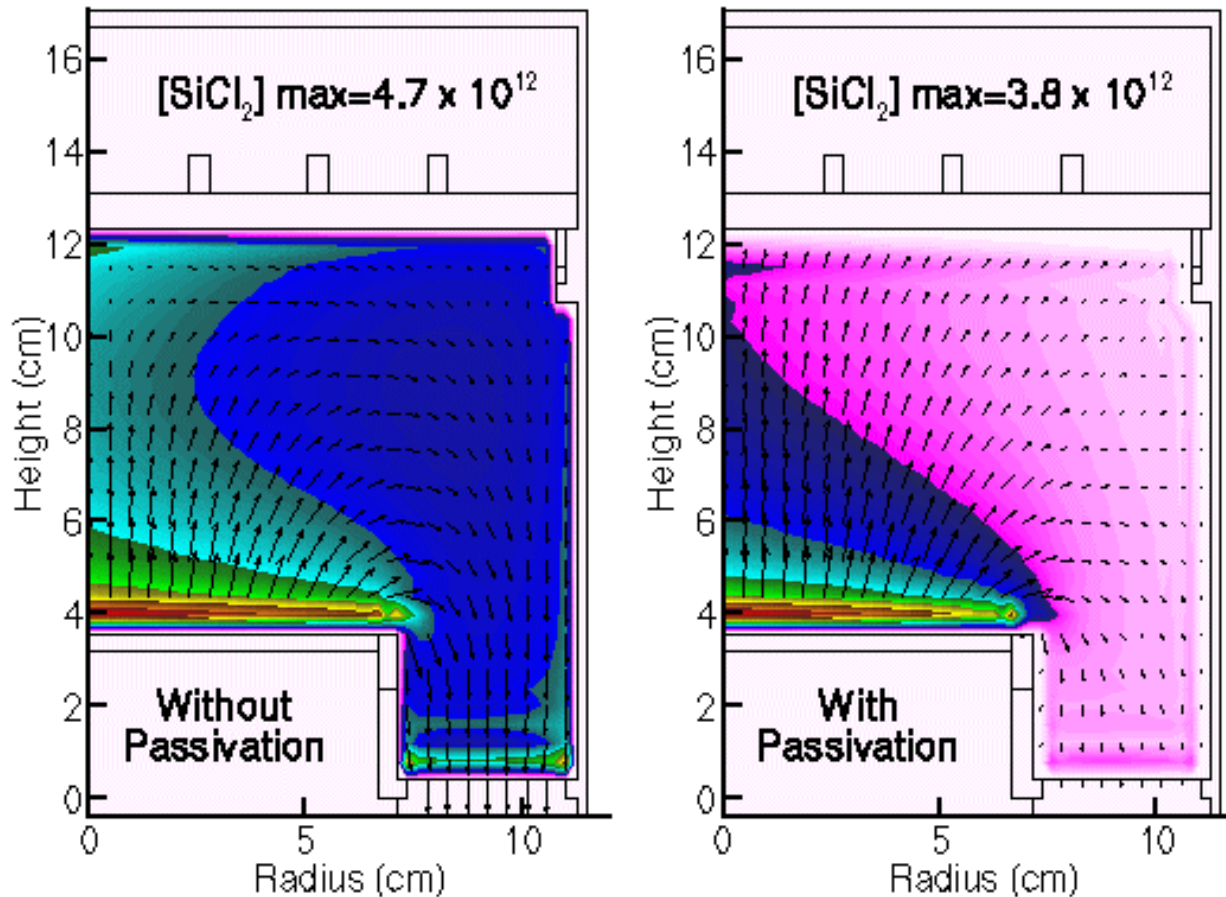
University of Illinois
Optical and Discharge Physics

CHEMICAL NONEQUILIBRIUM: Ar/Cl₂ WITH WALL PASSIVATION

- Computationally contrast Ar/Cl₂ ICPs etching Si with SiCl₂ product, with/without wall passivation.
- Implement a multistep passivation model beginning with SiCl₂ polymerization. Higher degree of polymerization reduces Cl reassociation.
- Without wall passivation: Cl → wall → Cl₂, p = 0.3
- With final wall passivation: Cl → wall → Cl₂, p = 0.01
- Ar/Cl₂ = 80/20, 10 mTorr, 400 W, 200 sccm

[SiCl₂] WITH/WITHOUT WALL PASSIVATION

- Without passivation, SiCl₂ has a longer residence time and builds to higher densities. Note momentum transfer from jetting nozzle.



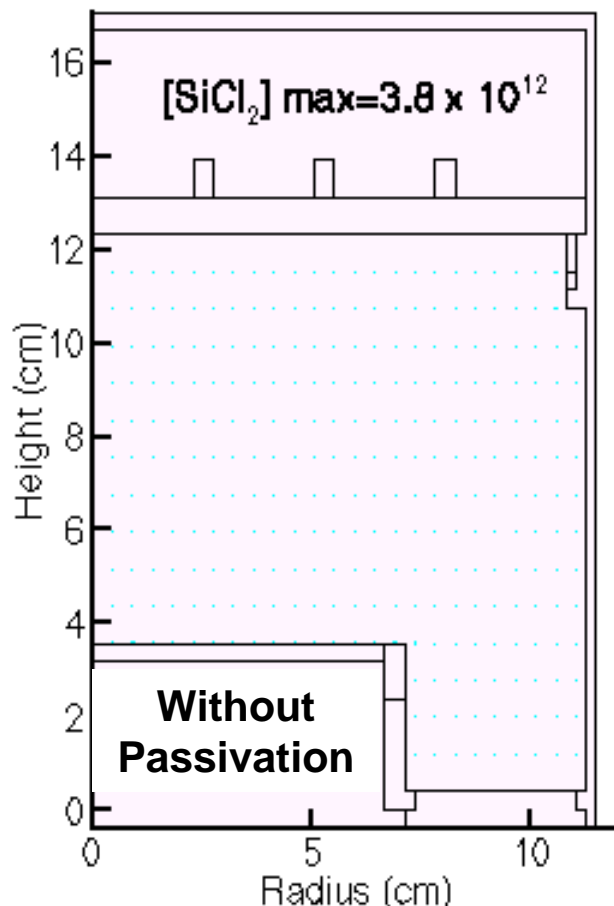
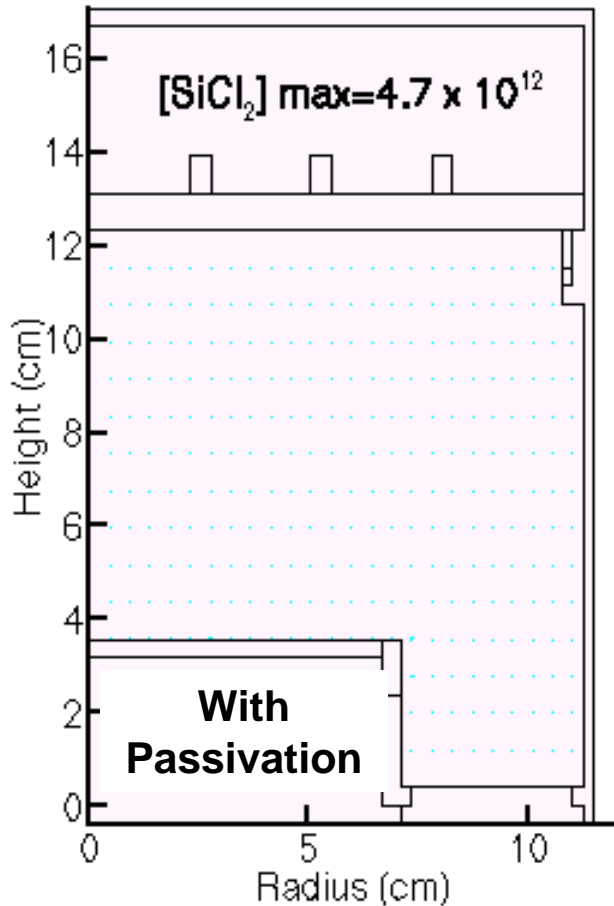
- Ar/Cl₂ = 80/20, 10 mTorr, 400 W, 200 sccm

MIN  MAX

University of Illinois
Optical and Discharge Physics

[SiCl₂] TRANSIENT WITH/WITHOUT WALL PASSIVATION

- SiCl₂ initially sticks to walls in both cases. As passivation progresses, the sticking coefficient decreases.



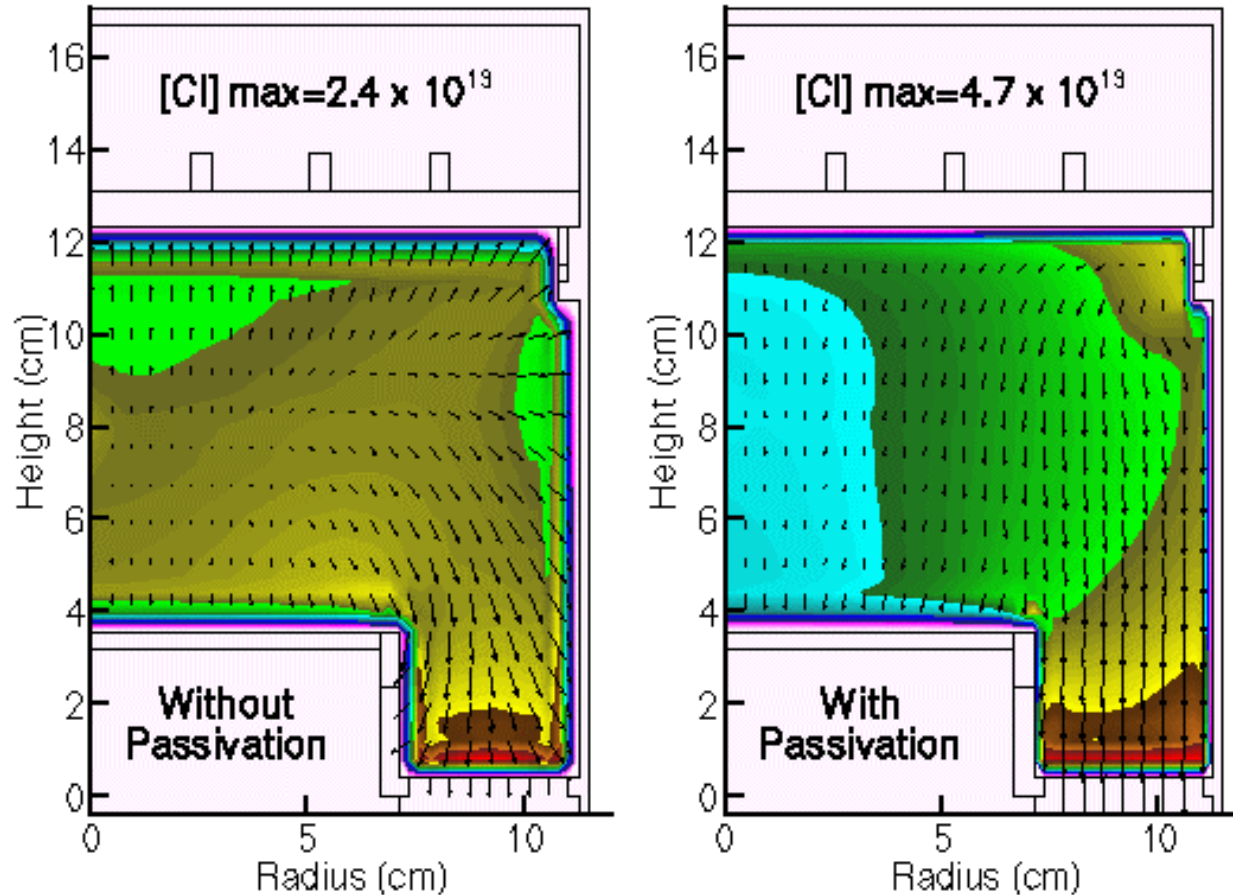
ANIMATION SLIDE

- Ar/Cl₂ = 80/20, 10 mTorr, 400 W, 200 sccm



[Cl] WITH/WITHOUT WALL PASSIVATION

- Passivation reduces Cl losses on the walls, increasing its density and making pumping the largest loss.



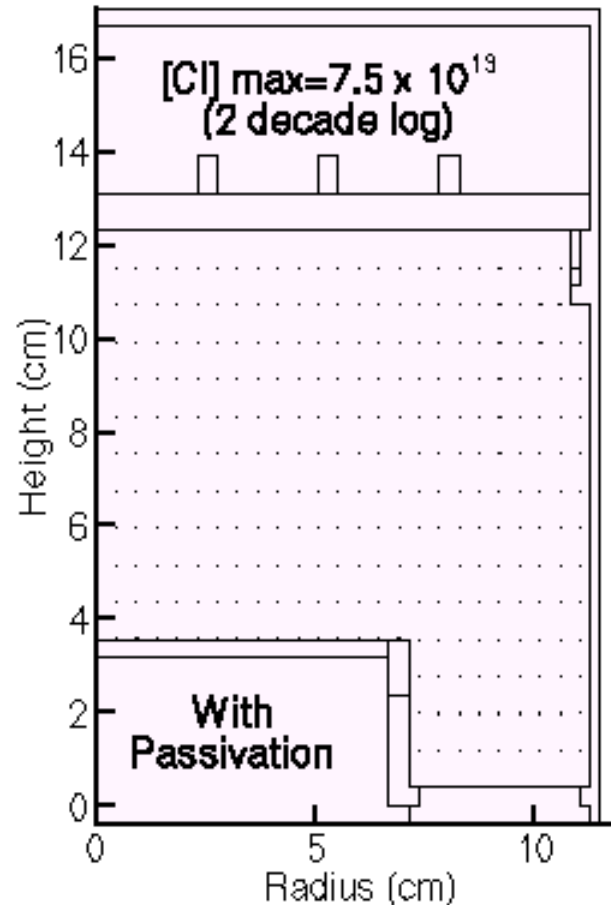
- Ar/Cl₂ = 80/20, 10 mTorr, 400 W, 200 sccm

MIN  MAX

University of Illinois
Optical and Discharge Physics

[Cl] TRANSIENT WITH WALL PASSIVATION

- When walls are clean, Cl reassociation is a large sink. As the walls passivate, surface losses decrease (except to wafer).



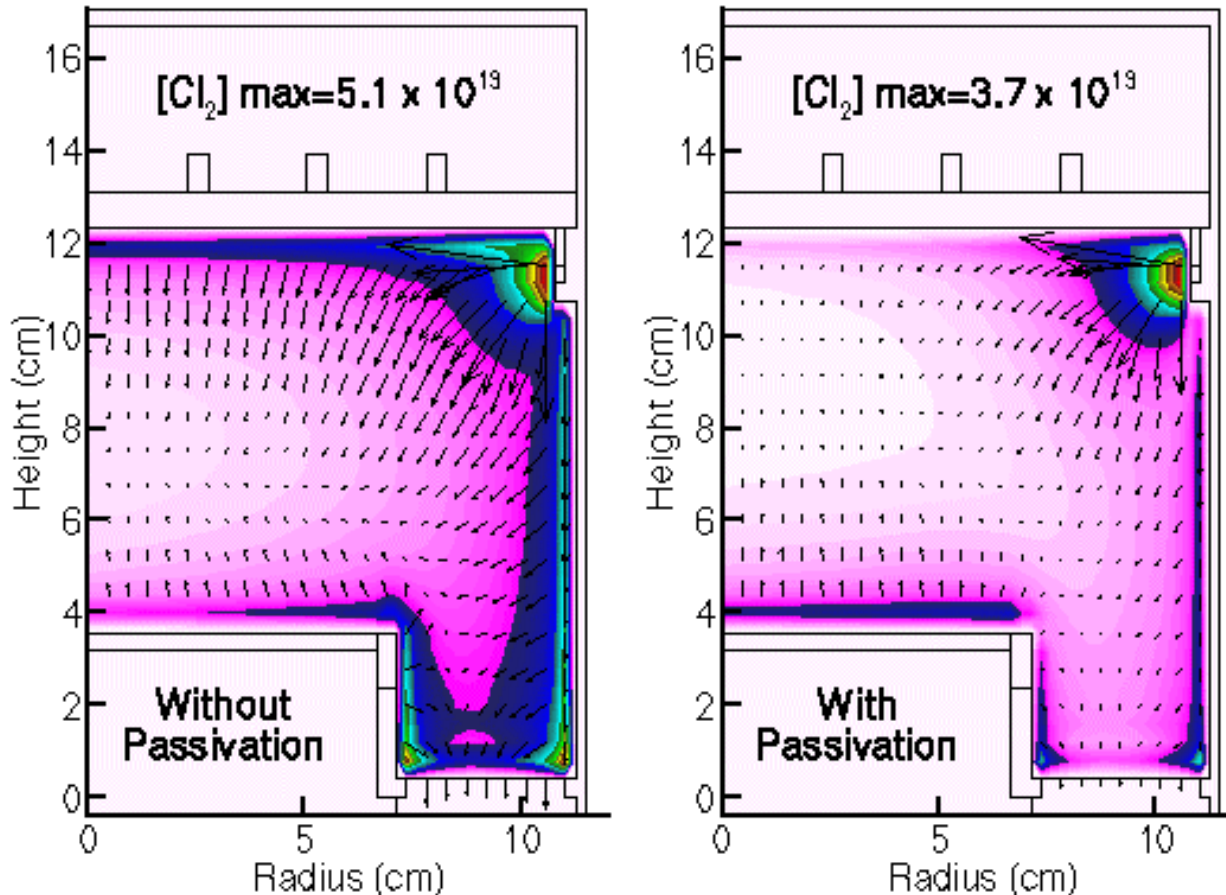
ANIMATION SLIDE

- $\text{Ar}/\text{Cl}_2 = 80/20$, 10 mTorr, 400 W, 200 sccm

MIN  MAX

[Cl₂] WITH/WITHOUT WALL PASSIVATION

- Without passivation, Cl₂ has sources at walls, raising its density. In both cases, dissociation fraction is large.



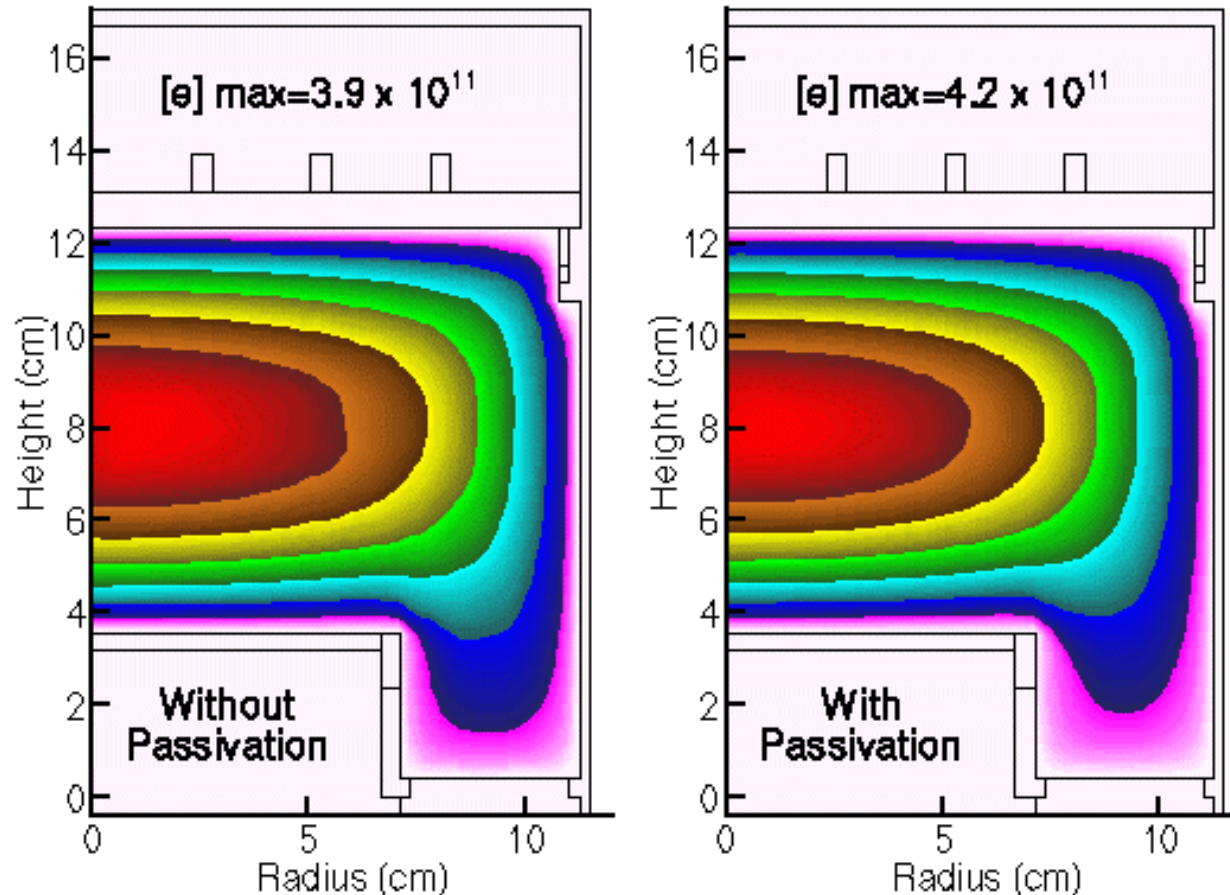
- Ar/Cl₂ = 80/20, 10 mTorr, 400 W, 200 sccm

MIN  MAX

University of Illinois
Optical and Discharge Physics

[e] WITH/WITHOUT WALL PASSIVATION

- Without wall passivation, sources Cl_2 from the walls are larger, resulting in more dissociative attachment and lower [e].



- $\text{Ar}/\text{Cl}_2 = 80/20$, 10 mTorr, 400 W, 200 sccm

MIN  MAX

University of Illinois
Optical and Discharge Physics

EXAMPLES OF NON-EQUILIBRIUM

- **Electromagnetic non-equilibrium: Anomalous skin depth**
- **Chemical non-equilibrium: Evolving wall passivation**
- **Electrostatic non-equilibrium: Microdischarges**

MICRODISCHARGE PLASMA SOURCES

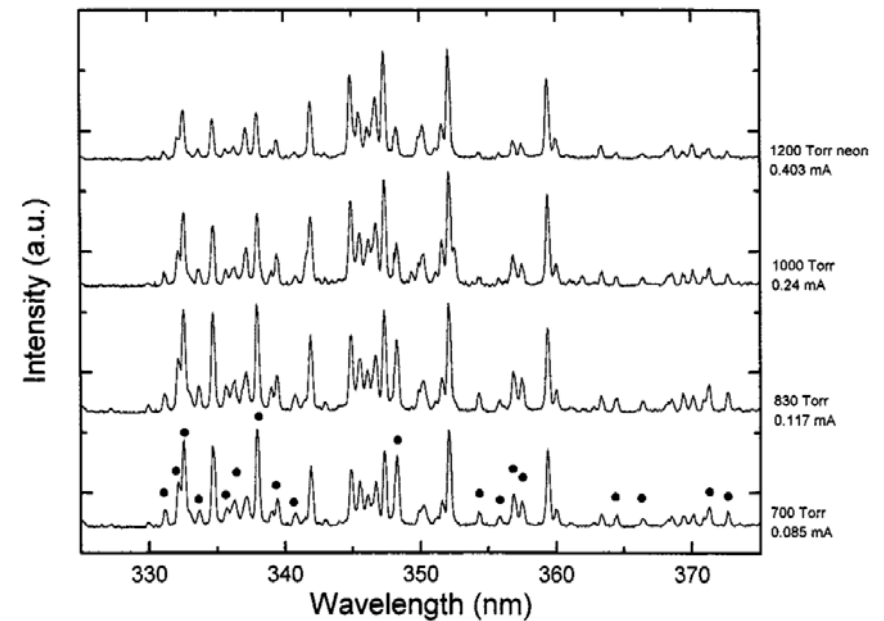
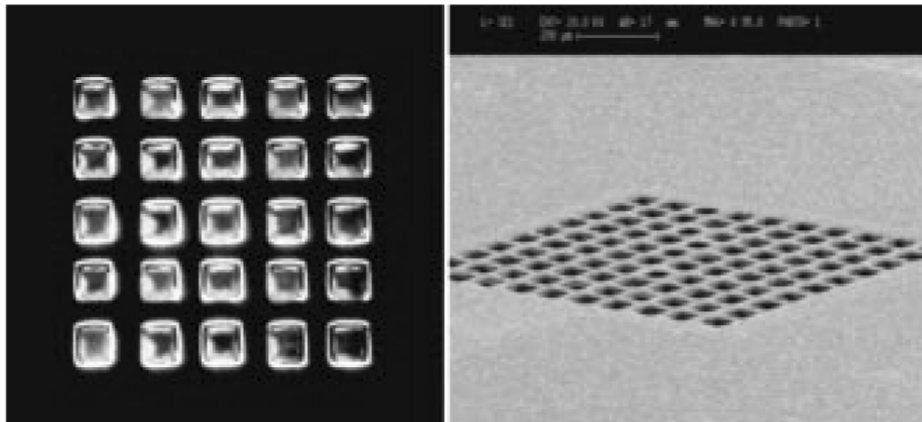
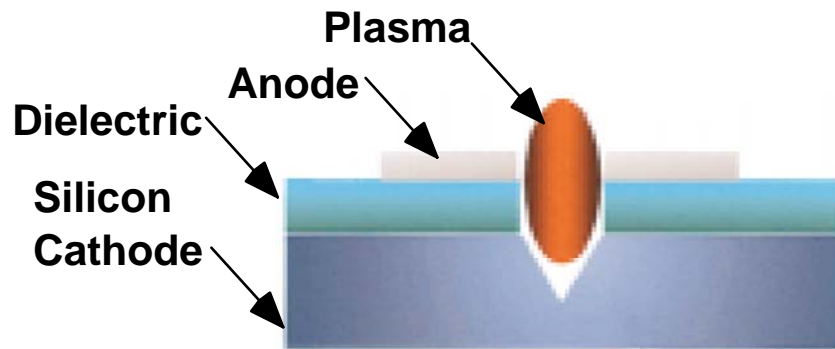
- Microdischarges are plasma devices which leverage pd scaling to operate dc atmospheric glows 10s –100s μm in size.
- MEMS fabrication techniques enable innovative structures for displays and detectors.
- Although similar to PDP cells, MDs are dc devices which largely rely on nonequilibrium beam components of the EED.
- Electrostatic nonequilibrium results from their small size. Debye lengths and cathode falls are commensurate with size of devices.

$$L_{\text{cathode Fall}} = \left(2V_c \epsilon_0 / (qn_I)\right)^{1/2} \approx 10 - 20 \mu\text{m}$$

$$\lambda_D \approx 750 \left(\frac{T_{eV}}{n_e (cm^{-3})} \right)^{1/2} cm \approx 10 \mu\text{m},$$

PYRAMIDAL MICRODISCHARGE DEVICES

- Si MDs with 10s μm pyramidal cavities display nonequilibrium behavior: Townsend to negative glow transitions.
- Small size also implies electrostatic nonequilibrium.



- S.-J. Park, et al., J. Sel. Topics Quant. Electron 8, 387 (2002); Appl. Phys. Lett. 78, 419 (2001).

University of Illinois
Optical and Discharge Physics

2-D MODELING OF MICRODISCHARGE SOURCES

- **Charged particle continuity (fluxes by Sharfetter-Gummel form)**

$$\frac{\partial N_i}{\partial t} = -\vec{\nabla} \cdot \left(qN_i \mu_i (-\vec{\nabla} \Phi) - D_i \nabla N_i \right) + S_i$$

- **Poisson's Equation for Electric Potential**

$$-\nabla \cdot \epsilon \nabla \Phi = \rho_V + \rho_S$$

- **Bulk continuum electron energy transport and MCS beam.**

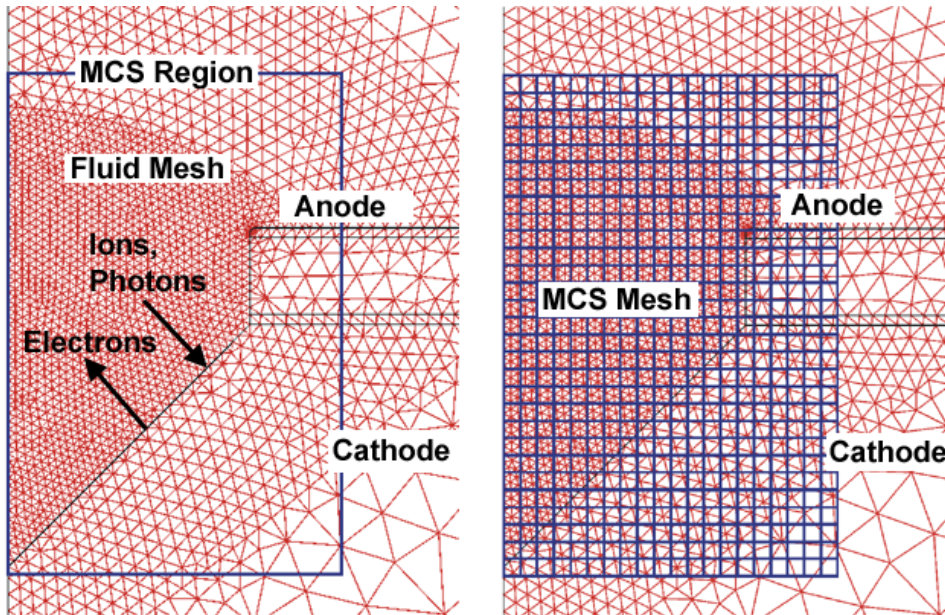
$$\frac{\partial (n_e \epsilon)}{\partial t} = \vec{j} \cdot \vec{E} - n_e \sum_i N_i \kappa_i - \nabla \cdot \left(\frac{5}{2} \epsilon \nabla \Phi - \lambda \nabla T_e \right), \quad \vec{j} = q \vec{\phi}_e$$

- **Neutral continuity and energy transport.**

$$\frac{\partial N_i}{\partial t} = -\nabla \cdot \left(\vec{v} - DN_o \nabla \left(\frac{N_i}{N_o} \right) \right) + S_i, \quad \frac{\partial (\rho c T)}{\partial t} = -\nabla \cdot \kappa \nabla T + P_g$$

DESCRIPTION OF MODEL: MCS MESHING

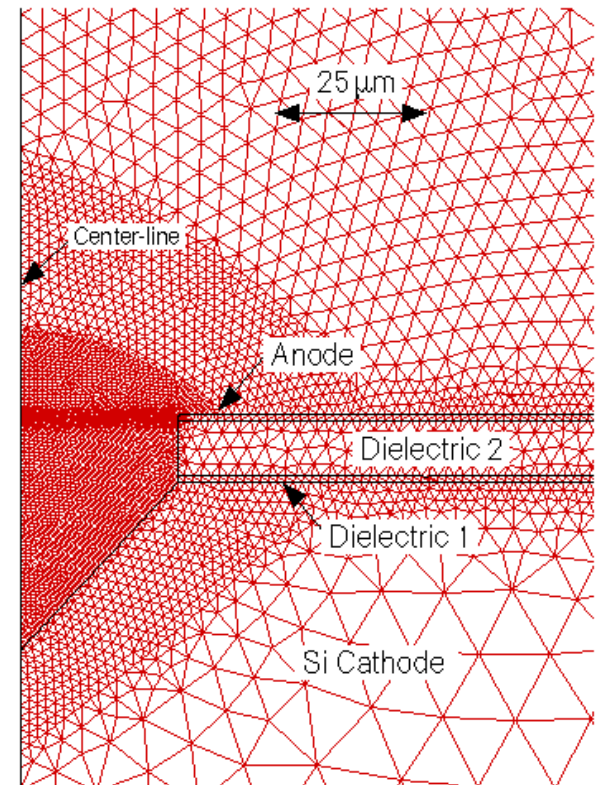
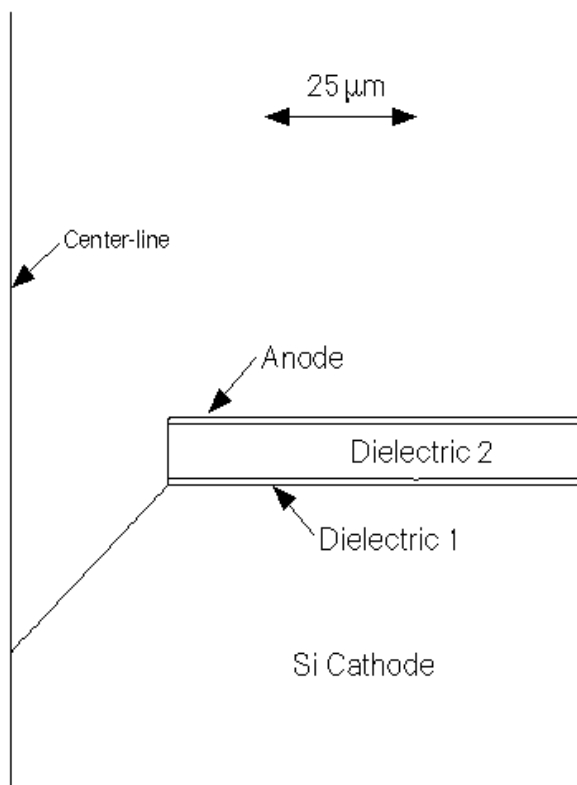
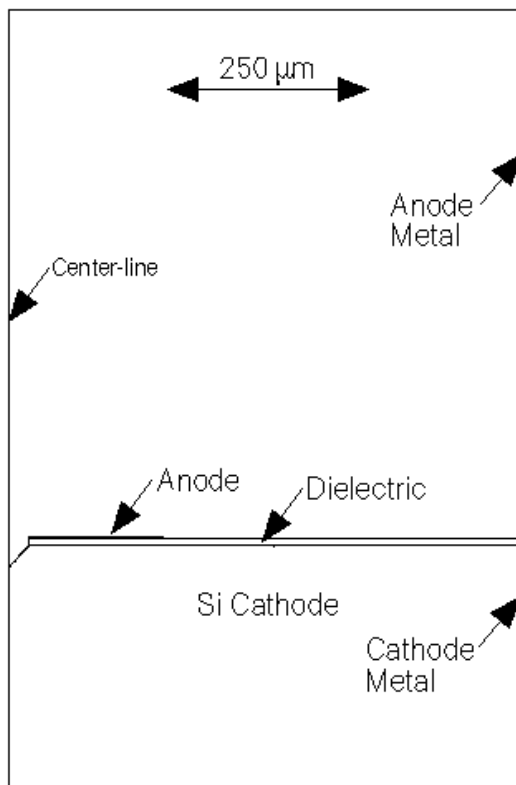
- Transport of energetic secondary electrons is addressed with a Monte Carlo Simulation.



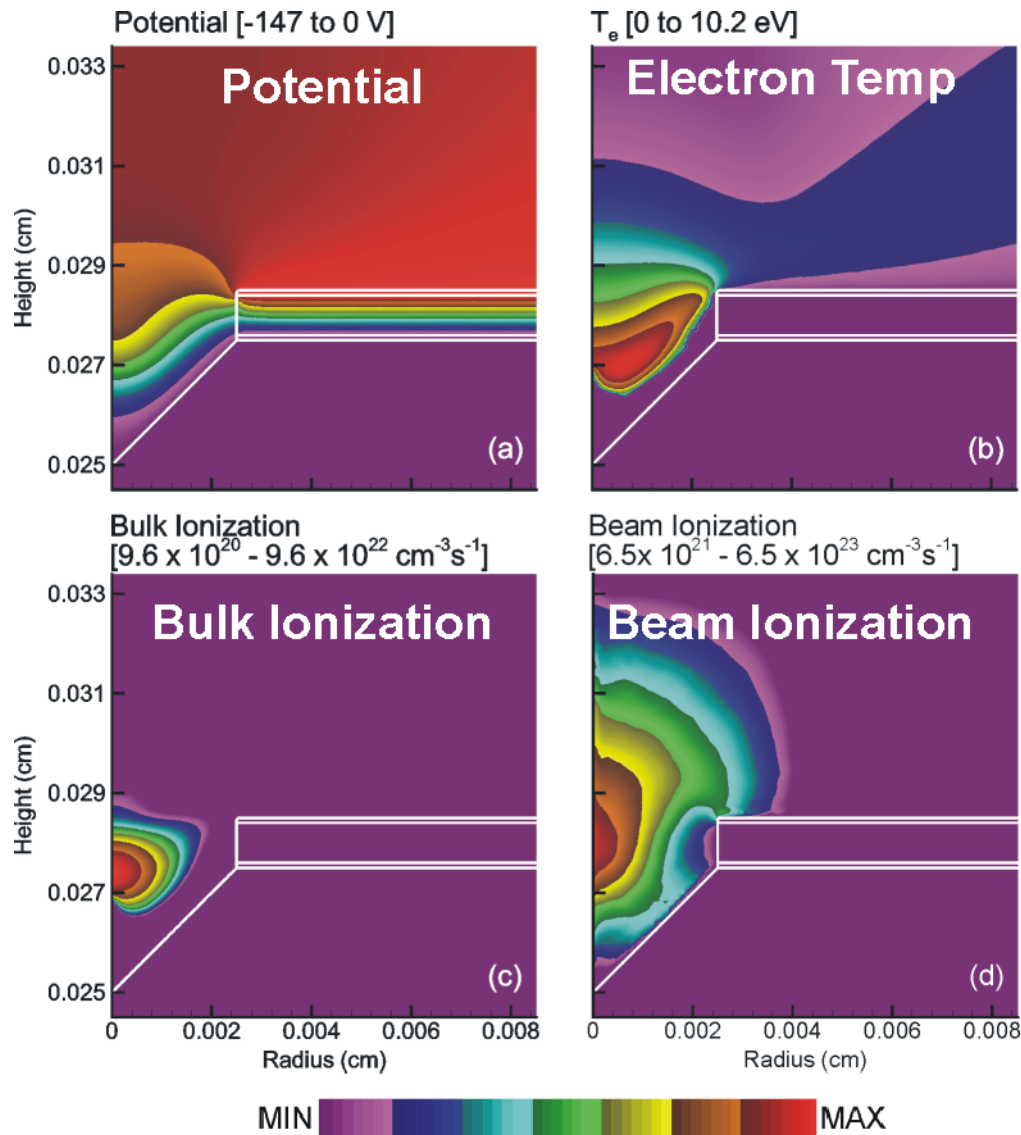
- Superimpose Cartesian MCS mesh on unstructured fluid mesh. Construct Greens functions for interpolation between meshes.
- Electrons and their progeny are followed until slowing into bulk plasma or leaving MCS volume.
- Electron energy distribution is computed on MCS mesh.
- EED produces source functions for electron impact processes which are interpolated to fluid mesh.

MODEL GEOMETRY: Si PYRAMID MICRODISCHARGE

- Investigations of a cylindrically symmetric Si pyramid MD.
Typical meshes have 5,000-10⁴ nodes, dynamic range of 50-100.



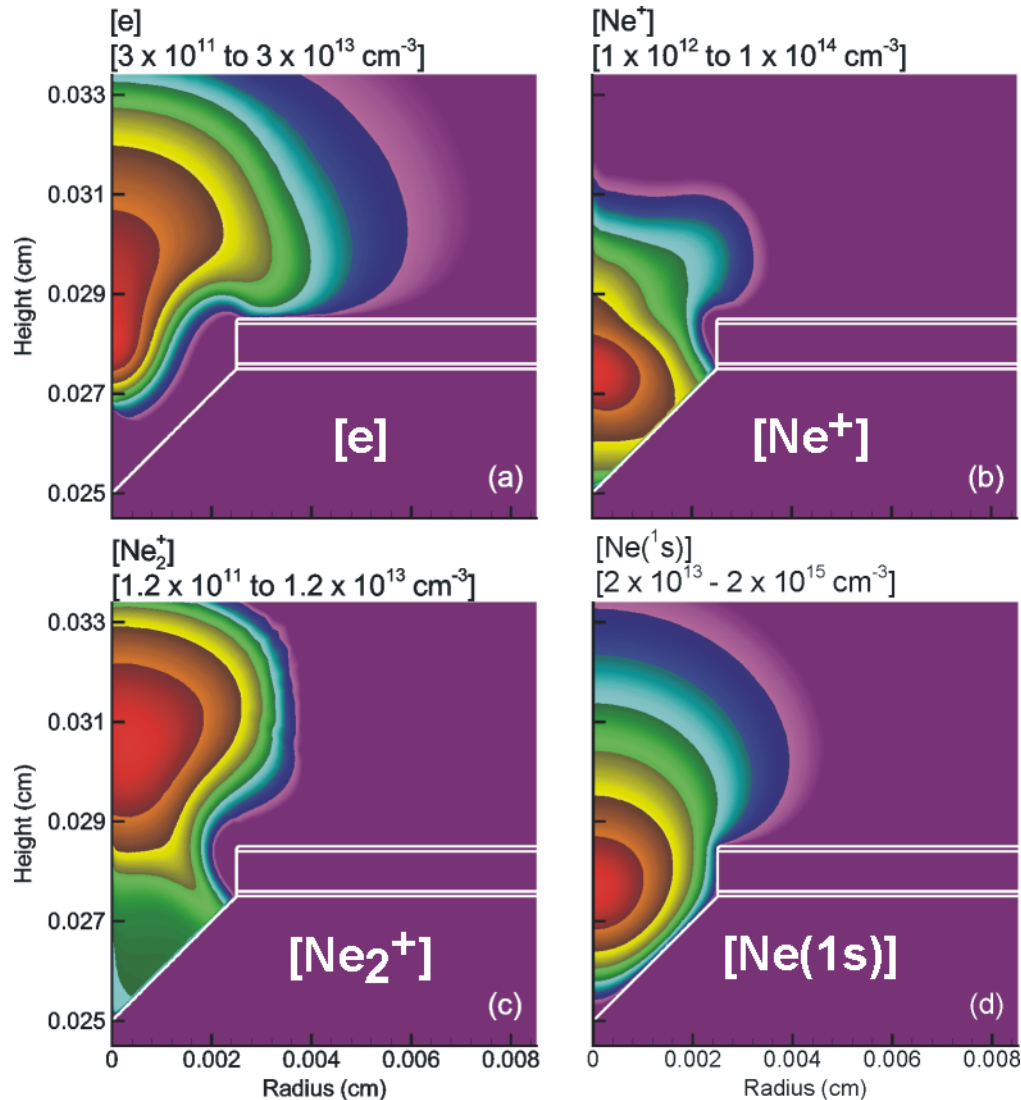
BASE CASE: Ne, 600 Torr, 50 μm DIAMETER



- Optimum conditions produces large enough charge density to warp electric potential into cathode well.
- In spite of large T_e , ionization is dominated by beam electrons.

• Ne, 600 Torr, 50 μm diameter, 200 V, 1 $\text{M}\Omega$

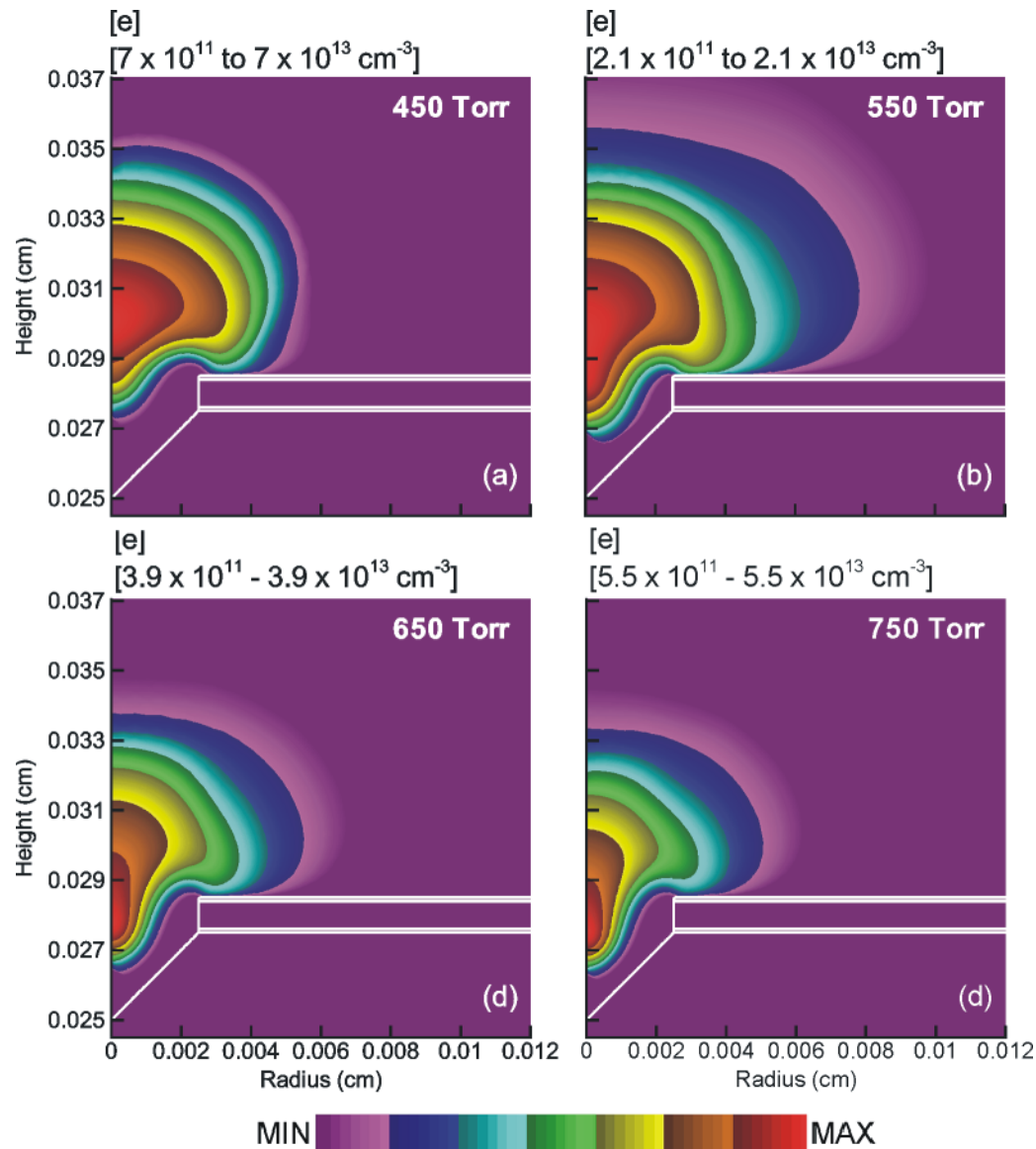
BASE CASE: CHARGED PARTICLE DENSITIES



- There are few regions of quasi-neutrality or which are positive column-like.
- $[e] > 10^{13} \text{ cm}^{-3}$ for 10s μA .
- Excited state densities $>10^{15} \text{ cm}^{-3}$ are commensurate with macroscopic pulsed discharge devices.

• Ne, 600 Torr, 50 μm diameter, 200 V, 1 M Ω

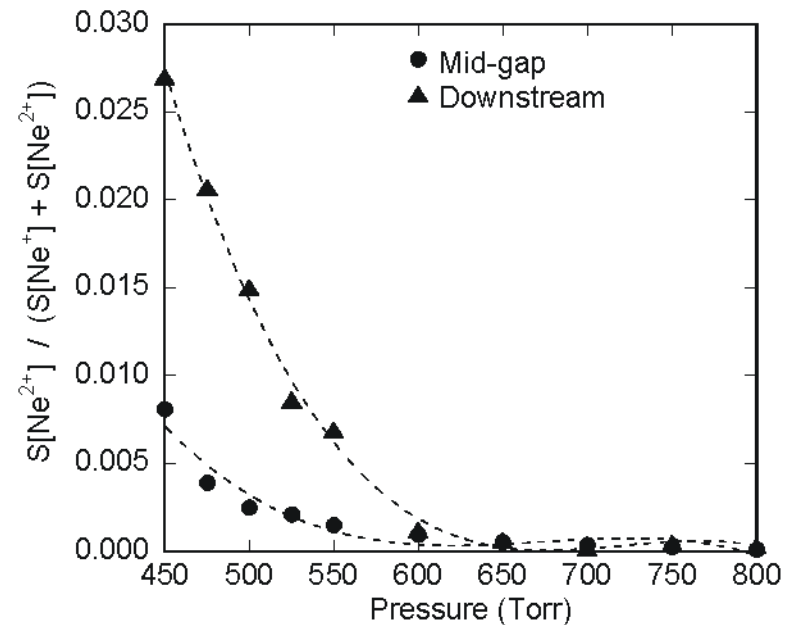
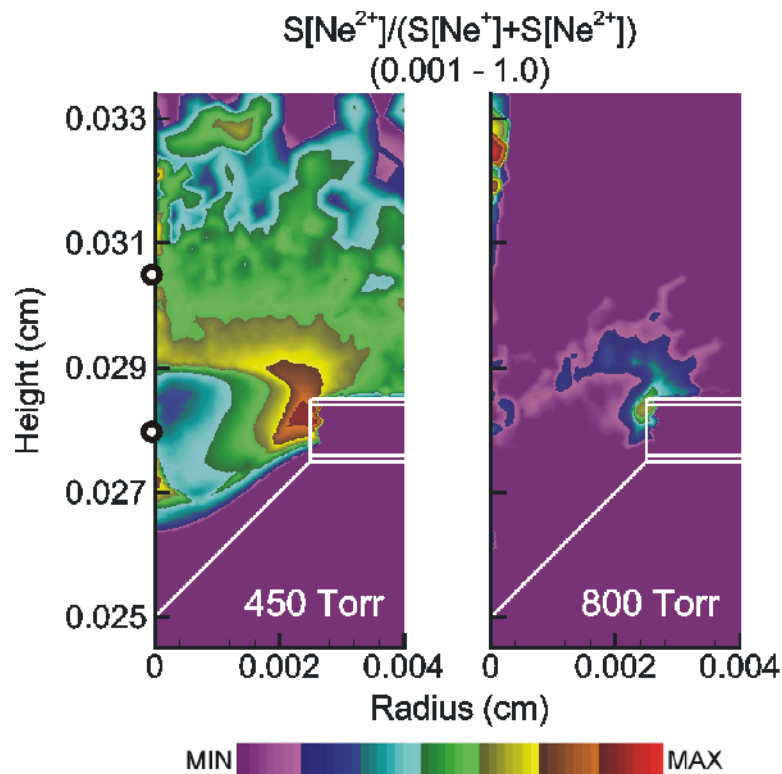
ELECTRON DENSITY vs PRESSURE



- The discharge becomes more confined at higher pressures due to shorter stopping length of beam electrons.
- Ne, 50 μm diameter, 200-240 V, 1 M Ω

BEAM vs BULK: NONEQUILIBRIUM IONIZATION SOURCES

- The threshold for $\text{Ne} \rightarrow \text{Ne}^{2+}$ is 41 eV. Monitoring $S[\text{Ne}^{2+}]/S[\text{Ne}^+]$ signals MD transitions from Townsend-like to negative glow-like.
- Negative glow-like excitation occurs with $P < 550$ Torr.

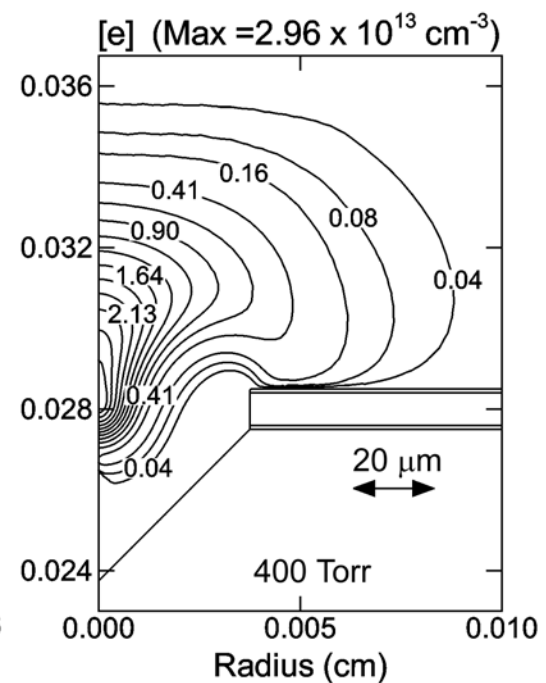
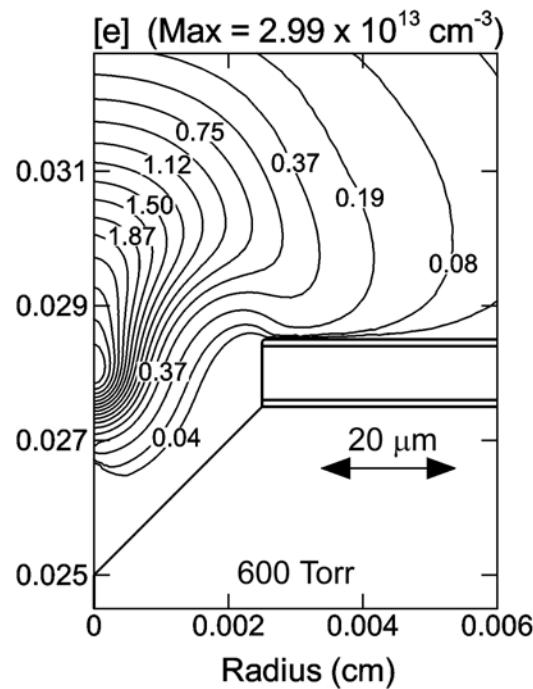
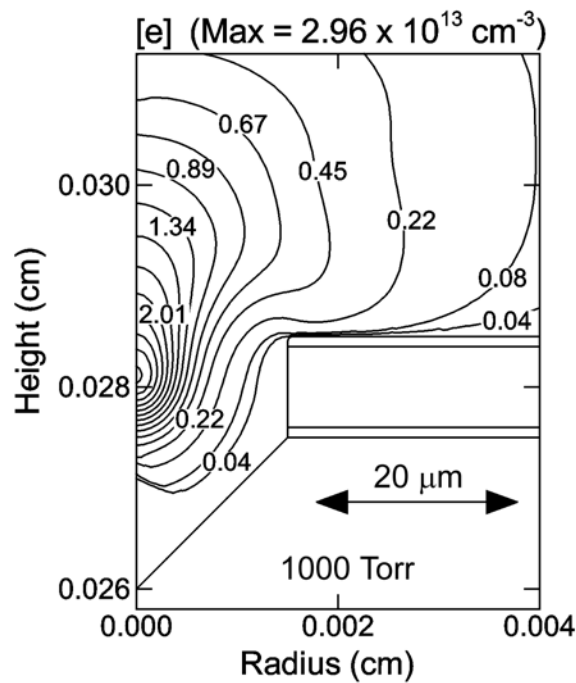


- Ne, 50 μm diameter, 200-240 V, 1 $\text{M}\Omega$

University of Illinois
Optical and Discharge Physics

SCALING WITH SIZE: $pd, j = \text{CONSTANT}$

- Pd scaling should not be a steadfast expectation.
- Sheath properties scale with absolute plasma density and not pd .
- Scaling requires careful ballasting to keep $[e]$ and sheath

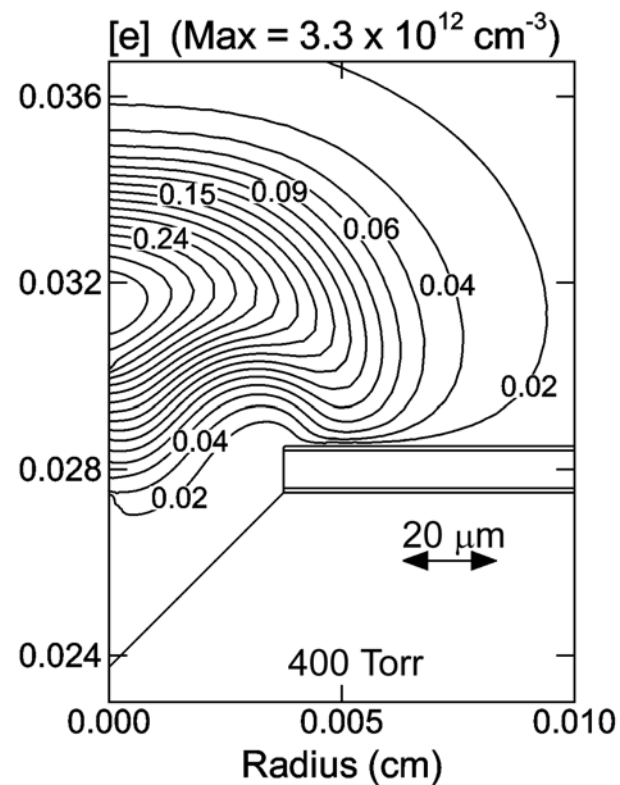
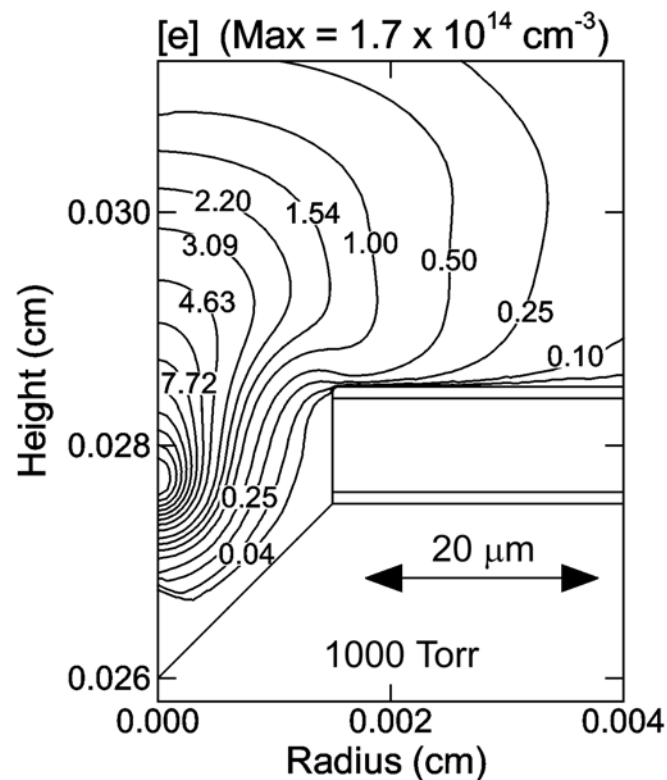


• Ne, 200 V, 1 M Ω

University of Illinois
Optical and Discharge Physics

SCALING WITH SIZE: pd, ballast = CONSTANT

- When keeping ballast constant, j decreases in larger devices, resulting in lower electron density, less shielding, more “electrostatic” equilibrium. Electron cloud “pops” out of cavity.



• Ne, 200 V, 1 M Ω

University of Illinois
Optical and Discharge Physics

CONCLUDING REMARKS and ACKNOWLEDGEMENTS

- **Nonequilibrium in plasma processing is everywhere you look...**
 - **Electromagnetics**
 - **Plasma dynamics**
 - **Surface chemistry**
 - **Electrostatics**
- **The development of computational and experimental techniques to resolve non-equilibrium will continue to be important in improving our fundamental understanding of these processes.**
- **Collaborators**
 - **Dr. Alex Vasenkov**
 - **Mr. Arvind Sankaran**